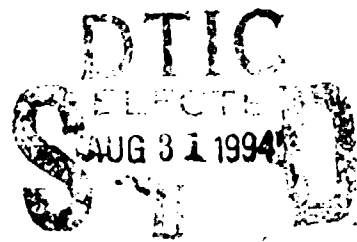Report No. NAWCADWAR-93010-60

STABILITY AND PERFORMANCE ROBUSTNESS
ASSESSMENT OF MULTIVARIABLE CONTROL SYSTEMS

Asok Ray, Jenny H. Shen, and Chen-Kuo Weng
Mechanical Engineering Department
THE PENNSYLVANIA STATE UNIVERSITY
University Park, PA 16802

APRIL 1993

DTIC
ELECTE
AUG 3 1 1994
S D

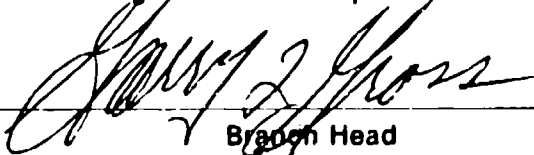*Approved for Public Release; Distribution is Unlimited*
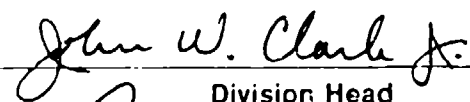
94 8 30 153

NOTICES

REPORT NUMBERING SYSTEM — The numbering of technical project reports issued by the Naval Air Warfare Center, Aircraft Division, Warminster is arranged for specific identification purposes. Each number consists of the Center acronym, the calendar year in which the number was assigned, the sequence number of the report within the specific calendar year, and the official 2-digit correspondence code of the Functional Department responsible for the report. For example: Report No. NAWCADWAR-92001-60 indicates the first Center report for the year 1992 and prepared by the Air Vehicle and Crew Systems Technology Department. The numerical codes are as follows:

CODE	OFFICE OR DEPARTMENT
00	Commanding Officer, NAWCADWAR
01	Technical Director, NAWCADWAR
05	Computer Department
10	AntiSubmarine Warfare Systems Department
20	Tactical Air Systems Department
30	Warfare Systems Analysis Department
50	Mission Avionics Technology Department
60	Air Vehicle & Crew Systems Technology Department
70	Systems & Software Technology Department
80	Engineering Support Group
90	Test & Evaluation Group

PRODUCT ENDORSEMENT — The discussion or instructions concerning commercial products herein do not constitute an endorsement by the Government nor do they convey or imply the license or right to use such products.

Reviewed By: _____ Date: 7/13/94
Branch Head

Reviewed By: _____ 7/13/94
Division Head

Reviewed By: _____ Date: 7/13/94
Director/Deputy Director

REPORT DOCUMENTATION PAGE

1. AGENCY USE ONLY (Leave blank)	2. REPORT DATE	3. REPORT TYPE AND DATES COVERED
	April 1993	Interim; 7/92 to 1/93

4. TITLE AND SUBTITLE	5. FUNDING NUMBERS
Stability and Performance Robustness Assessment of Multivariable Control Systems	Office of Naval Research Grant No. N00014-90-J-1513 (Extension)

6. AUTHOR(S)

Professor Asok Ray, Dr. Jenny H. Shen and Mr. Chen-Kuo Weng

7. PERFORMING ORGANIZATION NAME(S) AND ADDRESS(ES)	8. PERFORMING ORGANIZATION REPORT NUMBER
The Pennsylvania State University Mechanical Engineering Department University Park, PA 16802	

9. SPONSORING/MONITORING AGENCY NAME(S) AND ADDRESS(ES)	10. SPONSORING/MONITORING AGENCY REPORT NUMBER
Naval Air Warfare Center Aircraft Division Warminster, PA 18974-5000	NAWCADWAR-93010-60

11. SUPPLEMENTARY NOTES

12a. DISTRIBUTION/AVAILABILITY STATEMENT	12b. DISTRIBUTION CODE
Approved for Public Release; Distribution is Unlimited.	

13. ABSTRACT (Maximum 200 words)

This report presents the results of control systems analysis and their potential applications to control systems synthesis for high performance aircraft, and provides a proven, tractable and portable methodology to quantify the robust stability and performance of highly integrated digital fly-by-wire control systems. The H_∞-based μ-analysis approach has been recommended for quantitative evaluation of robust stability and performance of multi-input multi-output (MIMO) control systems. This approach for MIMO control systems evaluation is more effective than the algorithms based on gain margin and phase margin.

14. SUBJECT TERMS	15. NUMBER OF PAGES
Stability Robustness, Performance Robustness, μ-Analysis and μ-Synthesis	50
	16. PRICE CODE

17. SECURITY CLASSIFICATION OF REPORT	18. SECURITY CLASSIFICATION OF THIS PAGE	19. SECURITY CLASSIFICATION OF ABSTRACT	20. LIMITATION OF ABSTRACT
Unclassified	Unclassified	Unclassified	UL

This page is intentionally left blank

ACKNOWLEDGMENTS

This page is intentionally left blank

TABLE OF CONTENTS

LIST OF FIGURES AND TABLES

LIST OF SYMBOLS

$B\underline{\Delta}$ subset of $\underline{\Delta}$ with with norm bounded by unity, i.e., $B\underline{\Delta} = \{ \Delta \in \underline{\Delta} : \bar{\sigma}(\Delta) \leq 1 \}$
set of complex numbers

C set of complex numbers

$C^{n \times m}$ set of $n \times m$ complex matrices

$\bar{C}_+$ subset of C having non-negative real part, i.e., $\bar{C}_+ = \{ \gamma \in C : \mathrm{Re}(\gamma) \geq 0 \}$

d external disturbance

D diagonal scaling matrix

$\underline{D}$ set of diagonal scaling matrices

e unweighted performance variable

F number of full blocks in $\underline{\Delta}$

F_l lower linear fractional transformation

F_u upper linear fractional transformation

G actual plant transfer matrix

$\hat{G}$ nominal plant transfer matrix

I identity matrix

K controller transfer matrix

L diagonal perturbation matrix

m_i dimension of the full block Δ_i in $\underline{\Delta}$

M finite-dimensional, linear, time-invariant control system

M_s set of real rational, proper, stable transfer matrices

p input perturbation to the nominal plant model

Q block-diagonal unitary transformation matrix

$\underline{Q}$ set of block-diagonal unitary transformation matrices

r_i dimension of the repeated scalar block in $\underline{\Delta}$

R set of real numbers

S number of repeated scalar blocks in $\underline{\Delta}$

S sensitivity transfer matrix

T complimentary sensitivity transfer matrix

U orthogonal matrix

w weighted control

W_{del} uncertainty weighting matrix

W_p performance weighting matrix

x state vector

z weighted performance variable

α scalar constant

β gain matrix of L

Δ block diagonal matrix (structured uncertainty)

Δ_G stable perturbation

$\underline{\Delta}$ set of block diagonal matrices

$\underline{\Delta}_{sys}$ structured uncertainty for robust performance

Φ_{cl} closed-loop characteristic polynomial

Φ_{ol} open-loop characteristic polynomial

ξ output of the system M

λ eigenvalue

$\mu_{\underline{\Delta}}$ structured singular value with the given block structure $\underline{\Delta}$

ρ spectral radius

$\overline{\sigma}$ maximum singular value

Σ set of perturbed plants

$\Theta(\underline{\Delta})$ set of all block diagonal, stable real-rational transfer matrices, with block structure of $\underline{\Delta}$

Ξ set of all real-rational, proper, stable, transfer matrices

ω angular frequency in radians/second

ψ exogenous input to the system M

1. INTRODUCTION

The objectives of this report are to present the results of control systems analysis and their potential applications to control systems synthesis for high performance aircraft, and identify a proven, tractable and portable methodology to quantify the robust stability and performance of highly integrated digital fly-by-wire control systems. These systems are characterized by multiple distributed sensing, processing, and actuator elements interconnected by a time-division-multiplexed digital data bus layer. The aircraft division of Naval Air Warfare Center at Warminster, PA is supporting this research for developing an analytical methodology and associated tools to assess the stability and performance robustness of multi-input multi-output (MIMO), bus-organized digital flight control systems. The computation elements and subsystem modules within the control system may have a multi-rate structure, usually but not always, in a whole integer ratio. Task synchronization between these elements may range from no synchronization to synchronization at the CPU clock level.

This research project consists of two phases that are to be performed sequentially. The results of Phase 1 of the project are presented in this report which addresses the development of a robustness assessment methodology suitable for analyzing a generic class of MIMO, bus-organized flight control systems. The future work in Phase 2 is projected to deal with implementation and validation of the methodology developed in Phase 1. This implementation in Phase 2 should account for bus data delays, multiple distributed computation delays, and various degrees of synchronism (or lack thereof) between the distributed processing elements and the data bus. This report is intended to provide useful information to the engineers and scientists from different organizations of DoD, NASA, and leading aerospace companies.

The currently available theories and methodologies for robustness assessment of multi-input, multi-output (MIMO) systems have been reveiwed and thoroughly examined in this report. Recent literature has shown three major different approaches to address the robust stability and performance of MIMO control systems. The first approach relies on the structured singular value (μ) and H∞ analyses in the framework of Linear Fractional Transformations (LFT) of MIMO systems that are subjected to uncertainties with known bounds [Doyle (1982)] and [Safonov (1982)]. The concepts and fundamental results and applications of μ-analysis and μ-synthesis are presented in the publications of Doyle and his coworkers [Skogestad et al. (1988), Stein and Doyle (1991), Balas et al. (1991), Packard and Doyle (1993), Packard et al. (1993)]. The second approach [Yeh et al. (1985a), Molander and Willems (1980), Tao et al. (1991)] generalizes the definition and calculation of gain and phase margins for MIMO systems analogous to those for

single-input, single-output (SISO) systems. The third approach [Freudenberg and Looze (1986), Freudenberg (1990)] examines the relationship between the open loop gain and phase with respect to the closed loop sensitivity and complementary sensitivity functions for SISO systems, and then formulates heuristic rules for shaping the loop transfer functions for MIMO systems. We have emphasized the first approach of μ-analysis for robustness assessment of MIMO systems, which constitutes the main body of this report. A simulation example has been provided to illustrate its usage. However, technical discussions on the second and third approaches are presented in the appendices without any simulation examples.

The stability robustness tests for MIMO systems starts with the basic requirement that the nominal closed-loop system must be stable, which can be tested via the multivariable Nyquist stability theory. Furthermore, stability robustness tests are also based on the multivariable Nyquist theory which is briefly described in one of the appendices.

This report is organized in five sections and three appendices. Section 2 presents the basic concept of the structured singular value (μ) and its properties along with the techniques of μ-analysis and μ-synthesis. The results of simulation experiments for the flight control system of an advanced aircraft are discussed in Section 3 to illustrate the efficacy of the μ-analysis technique for MIMO systems. Section 4 describes the codes, developed in the MATLAB environment, which can be used for robustness analysis and synthesis of MIMO control systems. The last section summarizes and concludes the findings of this research report. Appendix A briefly describes the principle of multivariable Nyquist criterion which is essential for understanding the stability of closed loop control systems. Appendix B provides a general definition and computational methods for gain and phase margins of MIMO systems in a framework analogous to those for SISO systems. Appendix C describes the relationship between open loop gain and phase with respect to the closed loop sensitivity and complementary sensitivity functions for SISO systems, and then formulates heuristic rules for shaping the loop transfer functions for MIMO systems.

2. STRUCTURED SINGULAR VALUE (μ) ANALYSIS

This section introduces the technique of robustness analysis for MIMO control systems based on H_∞ and μ-analysis & synthesis.

2.1. The Structured Singular Value

Figure 2-1 shows how the plant perturbations represented by $\Delta(s)$, $s \in C$, interact with the finite-dimensional, linear, time-invariant control system $M(s) \in C^{n \times n}$ which is the based on the nominal plant model. The input ψ to the control system M consists of: all exogenous signals, namely, the reference command(s) to be tracked, disturbances and sensor noise; and the feedback control input. The output ξ of the control system M consists of: all plant variables needed for specifying the stability and performance criteria; and the sensor data feeding the controller. In the definition of the structured singular value $\mu_{\underline{\Delta}}(M(s_0))$ of the transfer matrix $M(s)$ at a given s_0, the underlying uncertainty $\Delta(s)$ belongs to a set of matrices, $\underline{\Delta}(s)$, which is prescribed to have a block diagonal structure with the following three characteristics:

- Type of each block;
- Total number of blocks;
- Dimension of each block.

In general, there are two types of blocks: Repeated scalar blocks and full blocks. Let two nonnegative integers, S and F, represent the number of repeated scalar blocks and the number of full blocks, respectively. We introduce positive integers, $r_1, ..., r_S; m_1, ..., m_F$, to represent the dimensions of these blocks such that

- The ith repeated scalar block is $\delta_i I_{r_i}$ where I_{r_i} is the $r_i \times r_i$ identity matrix and $\delta_i \in C$

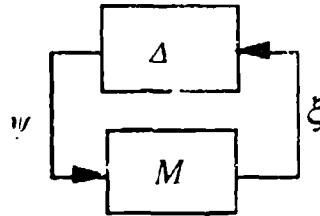- The jth full block belongs to $C^{m_j \times m_j}$.

Figure 2-1. The Closed-Loop Control system

Definition 1: The block diagonal structure, $\underline{\Delta}(s)$, is defined as:

$$\underline{\Delta}(s) = \left\{ diag\left[\delta_1(s)I_{r_1}, ..., \delta_S(s)I_{r_S}, \Delta_1(s), ..., \Delta_F(s) \right] : \delta_i \in C, \Delta_j \in C^{m_j \times m_j} \right\} \subset C^{n \times n} \qquad (1)$$

The following constraint must be satisfied for consistency of the dimensions:

$$\sum_{i=1}^{S} r_i + \sum_{j=1}^{F} m_j = n \tag{2}$$

The following notation is introduced in terms of norm-bounded subsets of $\underline{\Delta}$:

$$\mathbf{B}\underline{\Delta} = \{\Delta \in \underline{\Delta} : \overline{\sigma}(\Delta) \le 1\} \tag{3}$$

Definition 2: For any $M \in C^{n \times n}$, its structured singular value $\mu_{\underline{\Delta}}(M)$ is defined as:

$$\mu_{\underline{\Delta}}(M) \equiv \begin{cases} \dfrac{1}{\inf\{\overline{\sigma}(\Delta) : \Delta \in \underline{\Delta}, \det(I - M\Delta) = 0\}} \\[4mm] 0 \qquad \forall \Delta \in \underline{\Delta}, \det(I - M\Delta) \ne 0 \end{cases} \tag{4}$$

Remark 1: The physical significance of $\mu_{\underline{\Delta}}(M)$ can be interpreted following the feedback loop in Figure 2-1 where the loop equations are:

$$\xi = M\psi; \text{ and } \psi = \Delta\xi \tag{5}$$

As long as $I - M\Delta$ is nonsingular, the only solution for the loop equations is $\psi = \xi = 0$. However, if $I - M\Delta$ is singular, then there are infinitely many solutions, and the norms $\|\psi\|$ and $\|\xi\|$ can be arbitrarily large. Thus the feedback system becomes unstable. Hence, $(\mu_{\underline{\Delta}}(M))^{-1}$ is a measure of the smallest Δ belonging to a given class of uncertainty structure that causes instability of the above MIMO feedback loop. In other words, $(\mu_{\underline{\Delta}}(M))^{-1}$ is the size of the smallest "destabilizing" $\Delta \in \underline{\Delta}$ which satisfies the condition of $\det(I - M\Delta) = 0$. It follows from the MIMO Nyquist stability test (see Appendix A) that the zeros of $\det(I - M\Delta)$ are the closed-loop poles of the feedback system. Therefore, if $M = M(s_0)$ is a transfer matrix evaluated at a point s_0 in the complex plane, $(\mu_{\underline{\Delta}}(M))^{-1}$ is the size of the smallest allowable Δ which moves a closed-loop pole to that location s_0.

The structured singular value $\mu_{\underline{\Delta}}(M)$ of a transfer matrix M can be related to the familiar linear algebraic quantities if $\underline{\Delta}(s)$ is bounded for every $s \in C$ as seen below [Doyle et al. (1982)]:

Result 1: If $\underline{\Delta} = \{\delta I : \delta \in C\}(S = 1, F = 0, r_1 = n)$, then $\mu_{\underline{\Delta}}(M) = \rho(M)$ where $\rho(M)$ is the spectral radius of M.

Result 2: If $\underline{\Delta} = C^{n \times n}$ $(S = 0, F = 1, m_1 = n)$, then $\mu_{\underline{\Delta}}(M) = \overline{\sigma}(M)$ where $\overline{\sigma}(M)$ is the largest singular value of M.

Result 3: For a general $\underline{\Delta}$, the following inequality holds.

$$\left\{ \delta I_n : \delta \in C \right\} \subset \underline{\Delta} \subset C^{n \times n} \tag{6}$$

From the definition of μ, and Results 1 and 2 above, it follows that:

$$\rho(M) \leq \mu_{\underline{\Delta}}(M) \leq \overline{\sigma}(M) \tag{7}$$

Since the difference between ρ and $\overline{\sigma}$ can be very large, the bounds in Result 3 may not be sufficiently tight for evaluation of $\mu_{\underline{\Delta}}(M)$. The following result [Doyle (1982)] snows how these bounds can be refined by transformations on M that do not affect $\mu_{\underline{\Delta}}(M)$ but do affect ρ and $\overline{\sigma}$.

Result 4: The following property of $\mu_{\underline{\Delta}}(M)$ holds:

$$\mu_{\underline{\Delta}}(MQ) = \mu_{\underline{\Delta}}(QM) = \mu_{\underline{\Delta}}(M) = \mu_{\underline{\Delta}}\left(DMD^{-1}\right) \tag{8}$$

with $Q^* \in \underline{Q}$ $\qquad Q\Delta \in \underline{\Delta} \qquad \overline{\sigma}(Q\Delta) = \overline{\sigma}(\Delta Q) = \overline{\sigma}(\Lambda) \qquad D\Delta = \Delta D \tag{9}$

for any $\Delta \in \underline{\Delta}$, $D \in \underline{D}$ and $Q \in \underline{Q}$ where the sets $\underline{D}$ and $\underline{Q}$ are defined as:

$$\underline{D} = \left\{ diag\left[D_1, \dots, D_S, d_1 I_{m_1}, \dots, d_{F-1} I_{m_{F-1}}, I_{n_F} \right] : D_i \in C^{r_i \times r_i}, D_i = D_i^* > 0, d_j \in R, d_j > 0 \right\}$$

$$\underline{Q} = \left\{ Q \in \underline{\Delta} : Q^* Q = I_n \right\} \tag{10}$$

Furthermore the bounds of $\mu_{\underline{\Delta}}(M)$ in (7) can be tightened to

$$\underset{Q \in \underline{Q}}{max} \rho(QM) \leq \underset{\Delta \in B\underline{\Delta}}{max} \rho(\Delta M) = \mu_{\underline{\Delta}}(M) \leq \underset{D \in \underline{D}}{inf} \overline{\sigma}\left(DMD^{-1}\right) \tag{11}$$

It is shown that the lower bound in eq. (11) is an equality [Doyle (1982)]. Apparently, no analytical techniques exist to find the global maximum of the spectral radius $\rho(QM)$ although it may have local maxima. Thus local search cannot be guaranteed to obtain μ from its lower bound. The μ software package [Balas et al. (1991)] uses a slightly different algorithm to compute the lower bound. While there are open questions about its convergence, this algorithm usually works well and has proven to be an effective tool for approximate computation of μ.

The upper bound can be reformulated as a convex optimization problem so that the global minimum can be found in principle. Unfortunately, the least upper bound is not always equal to

μ. For block structures $\underline{\Delta}$ satisfying $2S + F \leq 3$, the least upper bound has been shown to be always equal to $\mu_{\underline{\Delta}}(M)$; and for block structures with $2S + F > 3$, μ may not attain the least upper bound. These results are summarized in the Table 2-1 to show for which cases the least upper bound is guaranteed to be equal to μ.

Table 2-1. Conditions for μ reaching its upper bound

S= \\ F=	0	1	2	3	4
0	—	yes	yes	yes	no
1	yes	yes	no	no	no
2	no	no	no	no	no

It is essential to estimate the upper and lower bounds for reliable use of the μ theory. The most important usage of the upper bound is in a computational scheme when it is combined with the lower bound. The other important feature of the upper bound is that it can be combined with H_∞ control synthesis methods to yield an iterative μ-synthesis method.

2.2. Linear Fractional Transformation

The dynamic system model in Figure 2-2 includes both parametric and non-parametric uncertainties where the complex matrix M of the nominal system is partitioned as:

$$M = \begin{bmatrix} M_{11} & M_{12} \\ M_{21} & M_{22} \end{bmatrix} \tag{12}$$

and the uncertainty block structure $\underline{\Delta}$ is compatible in size with M_{22}. For $\Delta \in \underline{\Delta}$, the loop equations are:

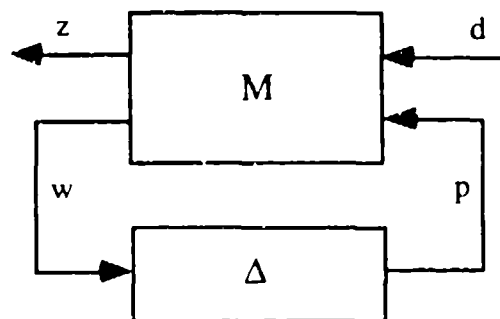$$z = M_{11}d + M_{12}p; \quad w = M_{21}d + M_{22}p; \quad \text{and} \quad p = \Delta w \tag{13}$$

Figure 2-2. Linear Fractional Transformation Structure

Definition 3: The system in Figure 2-2 is well-posed if there exist unique vectors z, w, and p such that the equation set (13) is satisfied for any exogeneous input vector d. In other words, the system is well-posed if and only if $I - M_{22}\Delta$ is invertible.

Remark 2: If the system in Figure 2-2 is not well-posed, then there are infinitely many solutions to the loop equation set (13).

Definition 4:: If the system in Figure 2-2 is well-posed, then the linear fractional transformation (LFT), $F_\ell(M,\Delta)$, on M induced by $\Delta \in \underline{\Delta}$ is defined as:

$$F_\ell(M,\Delta) = M_{11} + M_{12}\Delta(I - M_{22}\Delta)^{-1}M_{21}$$

and (14)

$$z = F_\ell(M,\Delta)d \text{ is satisfied.}$$

Remark 3: The subscript ℓ on F_ℓ pertains to the "lower" loop of M being closed by $\Delta \in \underline{\Delta}$ as shown in Figure 2-2. An analogous formula describes $F_u(M,\Delta)$, which is the resulting matrix obtained by closing the "upper" loop of M via an uncertainty matrix having z as the input and d as the output.

Remark 4: In the LFT formulation of eq. (14), the sub-matrix M_{11} represents the nominal plant transfer matrix; $\Delta \in B\underline{\Delta}$, as defined in eq. (3), can be viewed as a norm-bounded perturbation from an allowable set; and the sub-matrices M_{12}, M_{21} and M_{22} provide the information of how the parametric and non-parametric uncertainties influence M_{11}.

Given two defined block structures, $\underline{\Delta}_1$ and $\underline{\Delta}_2$, which are compatible in size with M_{11} and M_{22} respectively, a block structure $\tilde{\underline{\Delta}}$ is generated as:

$$\tilde{\underline{\Delta}} = \left\{ \begin{bmatrix} \Delta_1 & 0 \\ 0 & \Delta_2 \end{bmatrix} : \Delta_1 \in \underline{\Delta}_1, \Delta_2 \in \underline{\Delta}_2 \right\}$$ (15)

Now the structured singular value μ can be computed relative to the above three block structures, $\tilde{\underline{\Delta}}$, $\underline{\Delta}_1$ and $\underline{\Delta}_2$. In general, the following two problems are of interest:

- Determination of whether the LFT is well posed for all $\Delta_2 \in \underline{\Delta}_2$ with $\bar{\sigma}(\Delta_2) \leq 1$; and
- Evaluation of a scalar measure of the transfer matrix $F_\ell(M,\Delta_2)$ relative to the norm-bounded set of perturbations $\underline{\Delta}_2$.

To solve the above two problems by calculating the structured singular values (μ), we present two theorems ([Packard et al. (1993)] and Balas et al. (1991)]) which form the foundation of

μ-analysis and synthesis. In this respect, the following notations are used: $\mu_1(\bullet)$ is with respect to $\underline{\Delta}_1$, $\mu_2(\bullet)$ is with respect to $\underline{\Delta}_2$, and $\mu_{1,2}(\bullet)$ is with respect to $\underline{\Delta}$ as defined in eq. (15).

Theorem 1 (Theorem 3.4, Balas et al. (1991), p. 2-13): The LFT $F_\ell(M, \Delta_2)$ is well posed for all $\Delta_2 \in B\underline{\Delta}_2$ if and only if $\mu_2(M_{22}) < 1$.

Theorem 2 (Theorem 3.5, Balas et al. (1991), p. 2-13): $\mu_{1,2}(M) < 1$ if and only the following two conditions hold:

- $\mu_2(M_{22}) < 1$

$$\begin{array}{c} Max \quad \mu_1(F_\ell(M, \Delta_2)) < 1 \\ \Delta_2 \in B\underline{\Delta}_2 \end{array}$$

(17)

2.3. Review of μ in the Frequency Domain

The most well known use of μ as a robustness analysis tool is in the frequency domain. Let $M(s)$ be the nominal transfer matrix of a stable, multi-input, multi-output transfer function of a linear time-invariant control system. Given the block structure of all perturbations which are themselves dynamic systems having the structure of $\underline{\Delta}$, the problem is to determine the effects of these perturbations on the control system. To accomplish this task, first let Ξ denote the set of all real-rational, proper, stable, transfer matrices. Associated with any block structure $\underline{\Delta}$, let $\Theta(\underline{\Delta})$ denote the set of all block diagonal, stable real-rational transfer matrices, with block structure of $\underline{\Delta}$.

$$\Theta(\underline{\Delta}) = \left\{ \Delta(s) \in \Xi : \ s \in \overline{C}_+ \right\}$$

(18)
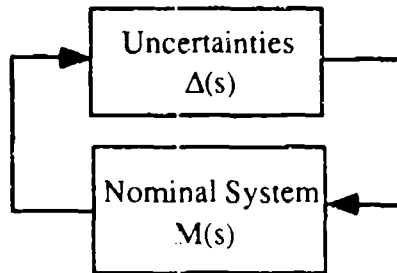

Figure 2-3. Linear Fractional Transformation in the Frequency Domain

Theorem 3 (Theorem 3.6, Balas et al. (1991), p. 2-14): For β>0, the feedback loop shown in Figure 2-3 is well-posed and internally stable for all $\Delta \in \Theta(\underline{\Delta})$ with $\|\Delta\|_\infty < \beta^{-1}$ if and only if

$$\left\| \mu_{\underline{\Delta}}(M) \right\|_{\infty} \equiv \frac{Sup}{\omega \in R} \mu_{\underline{\Delta}}(M(j\omega)) \leq \beta \qquad (19)$$

Remark 5:: Theorem 3 ensures that the peak value on the μ-plot of the frequency response corresponds to the perturbation whose size determines the robust stability of the loop system.

Often performance, in addition to stability of a closed-loop system, must be robust to perturbations. Typically there are exogenous disturbances acting on the system which result in tracking or regulating errors. Under the perturbation, the effects of these disturbances on the error signals can significantly increase and consequently the closed-loop system performance may not be acceptable. Therefore, a procedure for robust performance test is necessary. Such a test should indicate the worst case performance degradation associated with a given level of perturbations. If the transfer matrix M is stable, real-rational and proper with $n_p + n_d$ inputs, and $n_w + n_z$ outputs, then M can be partitioned such that M_{11} has n_p inputs and n_w outputs, M_{22} has n_d inputs and n_z outputs, and the remaining two submatrices of M have compatible dimensions. Let the block structure $\underline{\Delta}_1 \subset C^{n_w \times n_p}$ of the uncertainties corresponding to the system submatrix M_{11} be augmented as follows:

$$\underline{\Delta}_{sys} \equiv \left\{ \begin{bmatrix} \Delta_1 & 0 \\ 0 & \Delta_2 \end{bmatrix} : \Delta_1 \subset \underline{\Delta} \subset C^{n_w \times n_p} ; \Delta_2 \subset C^{n_z \times n_d} \right\} \qquad (2$$

The above block structure is set to address the robust performance of the loop shown in Figure 2-4, and the perturbed (closed loop) transfer matrix is denoted by $F_u(M, \Delta)$ with $\Delta(s) \in \Theta(\underline{\Delta}_{sys})$

Theorem 4: (Theorem 3.7, Balas et al. (1991), p. 2-16): Let $\beta > 0$. For all $\Delta(s) \in \Theta(\underline{\Delta}_{sys})$ with $\left\| \Delta \right\|_{\infty} < \frac{1}{\beta}$, the loop in Figure 2-4 is well-posed, internally stable, and $\left\| F_u(M, \Delta) \right\|_{\infty} \leq \beta$ if and only if

$$\left\| \mu_{\underline{\Delta}_{sys}}(M) \right\|_{\infty} \equiv \frac{sup}{\omega \in R} \mu_{\underline{\Delta}_{sys}}(M(j\omega)) \leq \beta \qquad (21)$$

In general, a procedure for μ-analysis and μ-synthesis of a control system to assure robust performance design procedure involves several steps:

Step 1: Specification of the closed loop feedback structure.

Step 2: Specification of the modeling uncertainty and performance objectives in terms of frequency-dependent weighting matrices.

Step 3: Construction of open-loop interconnection for the control synthesis routines.

Step 4: Design of the controller for the open-loop interconnection in Step 3.

Step 5: Analysis of robustness properties of the resulting closed-loop systems using the structured singular value. known as μ-analysis.

Step 6: Identification of frequency-dependent matrices, obtained in the μ-analysis step, to scale the open loop interconnection.

Step 7: Redesign of the scaled H_∞ controller.

Step 8: Iteration, if necessary, on Steps 5, 6 and 7, known as μ-synthesis.

Figure 2-4. Transfer Matrix with Perturbations

2.4. The μ-Analysis:

The objective is to analyze a stabilizing controller K for all stable perturbations $\Delta_G(s)$, with $\|\Delta_G\|_\infty < 1$. The controller K must satisfy the following conditions:

• The perturbed closed-loop system remains stable

• The perturbed weighted sensitivity transfer matrix relating z to d

$$S(\Delta_G) \equiv W_p[I + \hat{G}(I + \Delta_G W_{del})K]^{-1} \tag{22}$$

has $\|S(\Delta_G)\|_\infty < 1$ for all such perturbations.

<u>Uncertainty Models</u>: Given the nominal plant transfer matrix $\hat{G}$, it is necessary to specify an uncertainty weighting matrix, W_{del}, and a normalized variable transfer matrix Δ_G. Both W_{del} and Δ_G have to be stable transfer matrices, and there must not be any pole-zero cancellation between W_{del}, Δ_G and $\hat{G}$ in the closed right-half plane. All of the uncertainties in modeling the plant should be captured in the normalized, variable transfer matrix Δ_G, which is used to parametrize the postulated differences between the nominal model, $\hat{G}$, and the actual behavior of the real plant denoted by $G = \hat{G}(I + \Delta_G W_{del})$ Therefore, the two transfer matrices W_{del} and Δ_G parametrize an entire set of plants which must be appropriately controlled by the robust controller K. The actual plant transfer matrix which includes the modeling errors and disturbances belongs to the following set:

$$\Sigma \equiv \{\hat{G}(I + \Delta_G W_{del}): \Delta_G \text{ stable}, \|\Delta_G\|_\infty \leq I\} \tag{23}$$

The performance of the closed loop nominal system is evaluated using the sensitivity matrix, $(I + \hat{G}K)^{-1}$ between the disturbance d and the performance variable z in Figure 2-4. The objective is to characterize good performance in terms of a weighted H_∞ -norm on this transfer matrix. Given a stable, real-rational transfer matrix W_p, the nominal performance is achieved if $\|W_p(I + \hat{G}K)^{-1}\|_\infty < 1$. Similar to the uncertainty model where the frequency-dependent weighting function W_{del} normalizes the specifications Δ_G for plant modeling uncertainties, the frequency-dependent weighting function W_p is used to normalize the performance such that the norm of the weighted sensitivity matrix is less than 1.

To analyze the controller of a given plant which is subjected to uncertainties, four different criteria need to be tested as explained below:

- <u>Nominal Stability</u>: The control system with the nominal plant in the loop is internally stable. That is, there are no pole-zero cancellations in the closed right-half s-plane, and the poles of the closed-loop system transfer matrix must lie in the open left-half s-plane.

- <u>Nominal Performance</u>: The performance objective is satisfied for the nominal plant model if:

$$\|W_p(I + \hat{G}K)^{-1}\|_\infty < 1 \tag{24}$$

- Robust Stability: The closed loop system between the perturbation p and the uncertainty weighted control $w = W_{del} u$ is internally stable for all possible plant models $G \in \Sigma$, i.e.,

$$\left\| W_{del} K\hat{G}(I + K\hat{G})^{-1} \right\|_{\infty} < 1 \tag{25}$$

- Robust Performance: The closed-loop system is internally stable for all $G \in \Sigma$ and, in addition, the performance objective is

$$\left\| W_p(I + GK)^{-1} \right\|_{\infty} < 1 \quad \forall G \in \Sigma \tag{26}$$

Remark 5: Referring to Figure 2-4, nominal performance can be equivalently expressed as:

$$\left\| M_{22} \right\|_{\infty} < 1 \tag{27}$$

and robust stability as:

$$\left\| \mu(M_{11}) \right\|_{\infty} < 1. \tag{28}$$

The following are the conditions of robust stability and performance:

$$\left\| \mu_1(M_{11}) \right\|_{\infty} < 1 \quad \text{and} \quad \underset{\Delta \in B\underline{\Delta}_I}{Max} \left\| \mu_2(F_u(M,\Delta)) \right\|_{\infty} < 1. \tag{29}$$

which, by Theorem 2, are equivalent to

$$\left\| \mu_{1,2}(M) \right\|_{\infty} < 1. \tag{30}$$

2.5. The µ–Synthesis

It follows from the µ analysis that the inequality $\mu_{1,2}(M) \leq \bar{\sigma}(DMD^{-1})$ holds for any diagonal matrix D with a block structure matching that of $\Delta = diag(\Delta_1,...,\Delta_n)$. In the µ-synthesis procedure [Packard and Doyle (1993)], the strategy is to pick stable diagonal transfer matrices $D(s)$ with stable inverses, then to use H_∞ synthesis to compute the controller K which minimizes $\left\| DF_\ell(\hat{G},K)D^{-1} \right\|_{\infty}$. The D -matrices may be either constants, with no state dynamics, or frequency dependent. The latter case would obviously increase the number of states in the synthesized controller K, and thereby add their states to those of the closed loop control system.

The µ–synthesis procedure can be executed, after the initial controller design, as a two-phase iterative process called the D-K iteration [Packard et al. (1993)] which is summarized below:

Phase 0: Design a controller $K(s)$ based on a given nominal plant transfer matrix (which may include the performance and stability weighting functions) such that the closed loop system is internally stable and satisfies the criteria of performance specifications.

Phase 1: Execute the μ-analysis procedure using the closed loop system. If the robustness requirement is not satisfactory, then pick a diagonal $D(s)$ so that $D(s)$ and $D^{-1}(s)$ are stable, and the upper bound $\overline{\sigma}(DF_l(\hat{G},K)D^{-1})$ is approximately minimized over the frequency range of interest.

Phase 2: Execute H_∞ synthesis to identify a controller $K(s)$ which minimizes the norm $\left\|DF_\ell(\hat{G},K)D^{-1}\right\|_\infty$ of the scaled system. Go back to Phase 1 and repeat the iterative procedure until the desired condition of $\mu_{1,2}(F_\ell(\hat{G},K)) < 1$ is achieved over the frequency range of interest or no further reduction in μ is possible.

3. A SIMULATION EXAMPLE

The (continuous-time) flight dynamic model [Safonov et al. (1981)] of an advanced aircraft, linearized at the operating condition of 7.62 kilometers and 0.9 Mach, was selected to illustrate the μ-analysis and μ-synthesis procedures. The plant matrices are given below.

$$
A = \begin{bmatrix}
-0.0226 & -36.6170 & -18.8970 & -32.0900 & 3.2509 & -0.7626 \\
0.0001 & -1.8997 & 0.9831 & -0.0007 & -0.1708 & -0.0050 \\
0.0123 & 11.7200 & -2.6316 & 0.0009 & -31.6040 & 22.3960 \\
0 & 0 & 1.000 & 0 & 0 & 0 \\
0 & 0 & 0 & 0 & -30.0000 & 0 \\
0 & 0 & 0 & 0 & 0 & -30.0000
\end{bmatrix}
$$

$$
B = \begin{bmatrix} 0 & 0 & 0 & 0 & 0 & 30 \\ 0 & 0 & 0 & 0 & 30 & 0 \end{bmatrix}^T, \qquad
C = \begin{bmatrix} 0 & 1 & 0 & 0 & 0 & 0 \\ 0 & 0 & 0 & 1 & 0 & 0 \end{bmatrix}
$$

The six plant state variables are forward speed, angle of attack, pitch rate, attitude angle, elevon actuator position, and canard actuator position; the two control inputs are elevon and canard signals; and the two output variables are angle of attack and attitude angle. The open loop plant poles are given in the Table 3-1.. Therefore, the nominal plant is unstable in the open loop with a pair of complex eigenvalues in the right-half s-plane.

Table 3-1. Plant open-loop poles

Open-loop poles of the plant
-5.6754 6.9002e-1+2.48e-1i 6.9002e-1-2.48e-1i -2.5794e-1 -3e+1 -3e+1

A diagram of the closed-loop system, which includes the feedback structure of the plant and the controller, and elements associated with the uncertainty models and performance objectives, is shown in Figure 3-1.

The dashed box represents the actual plant, with associated transfer function G. Inside the box is the nominal model of the airplane dynamics, $\hat{G}$, and two elements, W_{del} and Δ_G, which represent the uncertainties in the plant model. The frequency weighting function W_{del} is assumed

to be known and reflects the amount of uncertainty in the model. The transfer matrix Δ_G is assumed to be stable and unknown, except for the norm condition, $\|\Delta_G\|_\infty < 1$. The performance objective is that the transfer matrix from d to z be small, in the $\|\bullet\|_\infty$ sense, for all possible uncertainty transfer matrices Δ_G. The weighting function W_p reflects the relative importance of various frequency ranges for which the performance is desired.
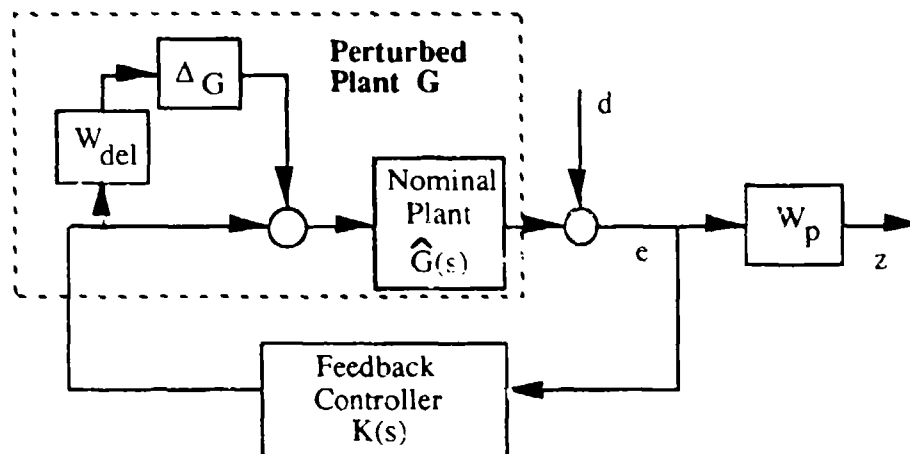

Figure 3-1. Closed-Loop System of the Aircraft Control with Uncertainties

The control objective is to identify a stabilizing controller K such that for all stable perturbations $\Delta_G(s)$, with $\|\Delta_G\|_\infty < 1$, the perturbed closed-loop system remains stable, and the perturbed weighted sensitivity transfer matrix,

$$S(\Delta_G) \equiv W_p(I + \hat{G}(I + \Delta_G W_{del})K)^{-1}$$

has $\|S(\Delta_G)\|_\infty < 1$. It follows from Section 2 that these objective functions are compatible to the structured singular value framework.

To formulate the problem into the framework of μ-analysis, we augment the perturbed plant as the open-loop system structure of p_block shown in Figure 3-2.

At the initial stage, we used three conventional algorithms for multivariable control systems synthesis, namely, LQG, H_2, and H_∞. Our intention was to compare the robustness of these three controllers under the same structure and bound of uncertainty blocks and disturbance blocks, and then formulate a strategy for quantitative evaluation of robust stability and performance. The results are summarized below.
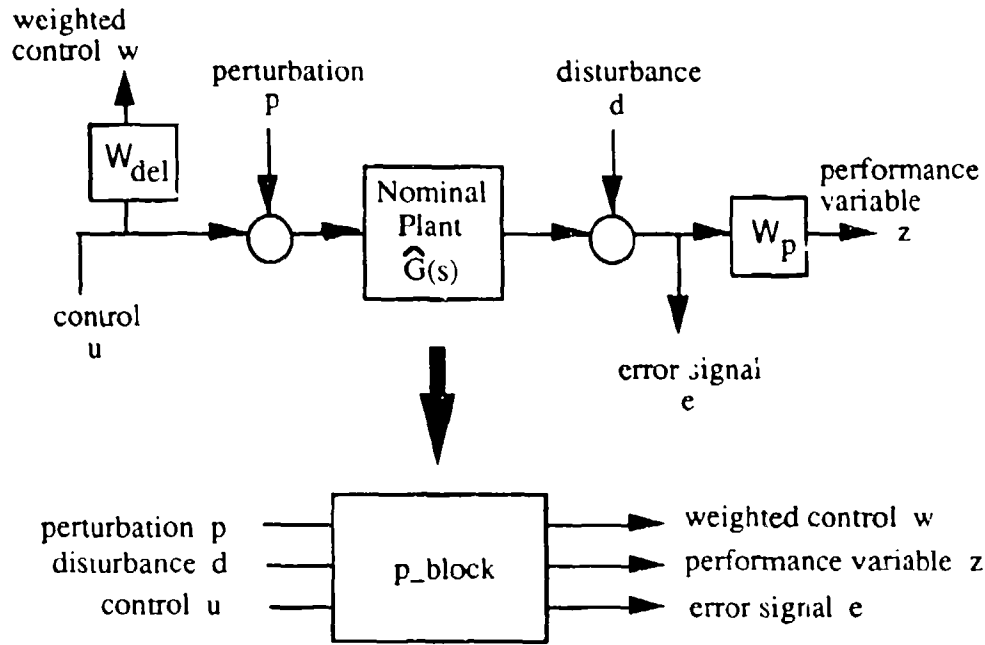
Figure 3-2. Augmented Open-Loop System

3.1. The LQG Controller

In the LQG synthesis, it is well known that the nominal closed-loop system is stable when controlled by the LQG compensator. The closed-loop poles of the nominal system are given in Table 3-2 for the state weighting matrix $Q_c=C^TC$; control weighting matrix $R_c=I_2$; plant noise covariance matrix $Q_f=BB^T$; and measurement noise covariance matrix $R_f=10^{-3}I_2$. As the nominal plant model was augmented with the modeling uncertainty blocks, the resulting closed loop system under LQG control became unstable. The closed loop poles are shown in Table 3-3. This instability results from the uncertainties imposed on the nominal plant. In that case, the loop transfer matrix from perturbation p to weighted control w in Figure 3-2 (after closing the loop with the LQG compensator) is:

$$w = K(s)(I - \hat{G}(s)K(s))^{-1}\hat{G}(s)p$$

The LQG system does not guarantee that the closed-loop system will remain stable in the presence of uncertaintes and disturbances [Doyle (1978)] although LQR guarantees a gain margin of $(\frac{1}{2},\infty)$ and phase margin of $(-60^o,+60^o)$. In this particular case, the output becomes easily unbounded because $\hat{G}(s)$ is unstable in the open loop.

Table 3-2. Closed-loop poles by LQG Design with Exact Parameters

Table 3-3. Closed loop poles by by LQG Design with Uncertain Parameters

Closed-loop poles by LQG design		Closed-loop poles of augmented structure
$\lambda(A - BF)$	$\lambda(A - LC)$	
-5.8348+4.4879i -5.8348-4.4879i -1.3878 -3.0056e+1 -3.00e+1	-20.199+28.714i -20.199-28.714i -4.2003e+1 -2.1404e-2 -2.6961 -2.9910e+1	-21.444+37.699i -21.444-37.699i -5.2851e+1 7.3409 -6.3281 -2.7026 -2.9909e+1 -3.00e+1 -8.271e-1 -2.9987e+1 7.0703e-3 -2.1401e-2

3.2. H_2 and H_∞ Controller Analysis Using μ

Two controllers were synthesized via H_2 and H_- norm optimization to stabilize the augmented open-loop structure in Figure 3-2. Based on the plant model and the desired performance of the closed loop control system, the respective weighting matrices, W_{del} and W_p, for uncertainty and performance were chosen to be:

$$W_{del} = \begin{bmatrix} \dfrac{s+3}{s+300} & 0 \\ 0 & \dfrac{s+3}{s+300} \end{bmatrix} \quad \text{and} \quad W_p = \begin{bmatrix} \dfrac{1}{s+0.03} & 0 \\ 0 & \dfrac{1}{s+0.03} \end{bmatrix}.$$

These two controllers were compared using the μ-analysis criteria described in Section 2. The selected set, S_D, of frequency points at which the control systems were analyzed and synthesized consists of $\ell = 60$ points logarithmically equally spaced between the decades of 10^{-3} to 10^4. The results for three different cases are shown in Tables 3-4, 3-5, and 3-6, respectively. The uncertainty and the external disturbances in Case 1 are represented by two full blocks, i.e., $\Delta_1 \subset C^{2\times2}$, and $\Delta_2 \subset C^{2\times2}$. This implies that the uncertain parameters in the plant could be perturbed arbitrarily in any form within a given bound. The parameter perturbation in the designed compensator is analogous to the concept of gain margin and phase margin in the SISO systems. As seen in Table 3-4, both H_2 and H_- controllers do not show good nominal and robust

performance ($\|M_{22}\|_\infty$ and $\max_{1\le i\le l} \mu(M(\omega_i))$ are larger than 1) although the H_∞ controller is superior to the H_2 controller from these perspectives. However, the stability robustness is good for both controllers because $\max_{1\le i\le l} \mu(M_{11}(\omega_i))$ is smaller than 1 for each.

Table 3-4. Comparison of the controllers (Case I)

Controller Algorithm	$\Delta_1 \subset C^{2\times2}$			$\Delta_2 \subset C^{2\times2}$	
	nominal performance	robust statibility		robust performance	
	$\|M_{22}\|_\infty$	$\max_{1\le i\le l}\mu(M_{11}(\omega_i))$	$\|\Delta_1\|_\infty$	$\max_{1\le i\le l}\mu(M(\omega_i))$	$\|\Delta\|_\infty$
H_2	2.5968	0.3237	3.0893	2.7834	0.3593
H_∞	1.5154	0.3234	3.0918	1.8184	0.5499

Table 3-5. Comparison of the controllers (Case II)

Controller Algorithm	$\Delta_1 = \{\delta I_2 : \delta \subset C^{2\times2}\}$			$\Delta_2 \subset C^{2\times2}$	
	nominal performance	robust statibility		robust performance	
	$\|M_{22}\|_\infty$	$\max_{1\le i\le l}\mu(M_{11}(\omega_i))$	$\|\Delta_1\|_\infty$	$\max_{1\le i\le l}\mu(M(\omega_i))$	$\|\Delta\|_\infty$
H_2	2.5968	0.3233	3.0936	2.6894	0.3718
H_∞	1.5154	0.3222	3.1035	1.6106	0.6209

Table 3-6. Comparison of the controllers (Case III)

Controller Algorithm	$\Delta_1 = \{diag[\delta_1,\delta_2] : \delta_1,\delta_2 \subset C^{2\times2}\}$			$\Delta_2 \subset C^{2\times2}$	
	nominal performance	robust statibility		robust performance	
	$\|M_{22}\|_\infty$	$\max_{1\le i\le l}\mu(M_{11}(\omega_i))$	$\|\Delta_1\|_\infty$	$\max_{1\le i\le l}\mu(M(\omega_i))$	$\|\Delta\|_\infty$
H_2	2.5968	upper: 0.3236 lower: 0.3236	3.0904	upper: 2.8917 lower: 2.7822	0.3594
H_∞	1.5154	upper: 0.3233 lower: 0.3233	3.0929	upper: 1.8896 lower: 1.8098	0.5525

Next, for Case II and Case III, the block $\underline{\Delta}_1$ was allowed to have two different structures while the full block structure of $\underline{\Delta}_2$ is unaltered. This can be interpreted as the plant uncertainty structure is changed but the external disturbances and the performance requirements remains unchanged. In Case II, it was assumed that $\underline{\Delta}_1 = \{\delta I_2 : \delta \in C\}$. This means that the uncertain parameters are only uniformly perturbed diagonally. In Case III $\underline{\Delta}_J = \left\{ \begin{bmatrix} \delta_I & 0 \\ 0 & \delta_2 \end{bmatrix} : \delta_I, \delta_2 \in C \right\}$ implies that the uncertain parameters are independently perturbed.

All three cases of μ-analysis in Tables 3-4, 3-5 and 3-6 show that both H_2 and H_∞ controllers possess reasonably good robust stability but not good nominal and robust performance. However, the H_∞ controller has a better nominal and robust performance. On the other hand, the robust performance of the H_∞ controller is sensitive to the uncertainty structure change, and apparently its robust performance should improve if the parameters are perturbed uniformly and diagonally.

The μ-analysis package [Balas et al. (1991)] is capable of calculating the upper and lower bounds of μ. As mentioned in Section 2, the lower bound μ is not exact although theoretically an equivalence exists. The upper bound of the exact μ can be reached for only some specified uncertainty structures as seen in Table 2-1. The upper bounds of the numerically computed μ match the exact value of μ for $\underline{\Delta}_J \in C^{2 \times 2}$ and $\underline{\Delta}_J = \{\delta I_2 : \delta \in C\}$ in Tables 3-4 and 3-5, respectively. However, neither the upper bound nor the lower bound is guaranteed to match the exact value of μ as seen in Table 3-6 because for $\underline{\Delta}_J = \left\{ \begin{bmatrix} \delta_I & 0 \\ 0 & \delta_2 \end{bmatrix} : \delta_I, \delta_2 \in C \right\}$.

3.3. μ-Synthesis and D-K Iteration

The H_2 optimization provides a unique controller while H_∞ optimization uses an iterative procedure to obtain an approximate solution [Doyle et al. (1989)]. The μ-analysis could be used to guide the iterative process of H_∞ optimization, and this process is called the D-K iteration [Packard et al. (1993)]. As described in Section 2.5, any linear time-invariant finite-dimensional stabilizing controller can be used to initiate the D-K iteration. However, in the subsequent steps of D-K iteration, only H_∞ synthesis has been used to update the controller, and μ-analysis is used to evaluate the designed controller at each iteration. In the example of this report, the controller was initially designed via H_∞ optimization and, after two passes of D-K iteration, the updated controller exhibited significantly superior robustness properties. In each of the two passes, a 4th order polynomial fit was chosen for the scaling matrix $D(s)$. The results are summarized below in Table 3-7.

Table 3-7. Comparison of the initial and final controllers given by D-K iteration

D-K iteration number	$\underline{\Delta}_1 \subset C^{2 \times 2}$			$\underline{\Delta}_2 \subset C^{2 \times 2}$	
	nominal performance	robust statibiliity		robust performance	
	$\|M_{22}\|_\infty$	$\max\limits_{1 \leq i \leq l} \mu(M_{11}(\omega_i))$	$\|\Delta_1\|_\infty$	$\max\limits_{1 \leq i \leq l} \mu(M(\omega_i))$	$\|\Delta\|_\infty$
initial 0	1.5154	0.3234	3.0918	1.8184	0.5499
1	0.9157	0.1933	5.1742	1.0175	0.9828
final 2	0.6573	0.1592	6.2800	0.7509	1.3317

Table 3-7 shows that robust stability of the final controller is significantly enhanced since $\max\limits_{1 \leq i \leq l} \mu(M_{11}(\omega_i))$ is much smaller than 1. The nominal performance and robust performance are also significantly improved since both $\|M_{22}\|_\infty$ and $\max\limits_{1 \leq i \leq l} \mu(M(\omega_i))$ are made less than 1 in final version of the control system synthesis.

The perturbation data obtained from the initial controllei analysis were used to build the transfer matrix $\Delta_G(s)$. If the perturbation data obtained from the final controller analysis is used, the control loop closed by the initial controller may become unstable. The rationale is that the final controller has better stability robustness than the initial one so that $\|\Delta_G(s)\|_\infty$ of the final controller is greater than that of the initial controller.

Figures 3-3 and 3-4 show the frequency domain simulation of the initial H_∞ controller and final H_∞ controller, respectively, to compare their robust performance and stability. The plant transfer matrix is $G(s) = \hat{G}(s)[I + \Delta_G(s)W_{del}(s)]$, where $\Delta_G(s)$ is a stable, real-rational transfer matrix constructed according to the uncertainty perturbations obtained from the μ-analysis data. Since $\bar{\sigma}(\Delta_G(s)) = (\mu(M_{11}(s)))^{-1}$ $\forall s \subset S_D$ where S_D is the selected set of frequency points for numerical computation of μ, the closed-loop system has the worst case perturbations among the set of actual plant transfer matrices.

Figures 3-3 and 3-4 compare the singular values of the nominal loop transfer matrices and nominal sensitivity matrices, respectively. The loop with the final controller has better performance than that with the initial controller because the minimal singular values of the loop transfer matrices of the final controller is higher at the low frequency range. Another interesting point is that the range of singular values from maximum to minimum is much larger for the final

controller than that for the initial controller. It is important to note that the conventional robust performance rule is very conservative under the assumption that all the singular values at the low frequency range must be high. However, since the final controller is constructed based on the μ theory, it is much less conservative than a controller synthesized via the conventional techniques. So the robustness constraints are relaxed and each singular value can be varied within a large range while the performance of the final controller as shown in Figure 3-3 is still higher. On the other hand, the maximum singular value of the loop transfer matrix of the final controller is higher than that of the initial controller. But the robust stability of the final controller, as shown in Table 3-7, is better than that of the initial controller. This is due to the same reason that μ-theory is much less conservative so that the stability bound for the nominal plant can be relaxed while keeping the stability robustness high. The example given in this report shows the difference between the nominal stability and robust stability, and the difference between the nominal performance and robust performance. For multivariable system controller analysis and synthesis, we should not only consider the nominal stability and performance but also the robust stability and performance. However, the benefit of the robustness is gained at the expense of an increased order of the controller in the D-K iteration. For real time implementation, a reduction of the controller model order [Balas et al. (1991)] might be necessary.
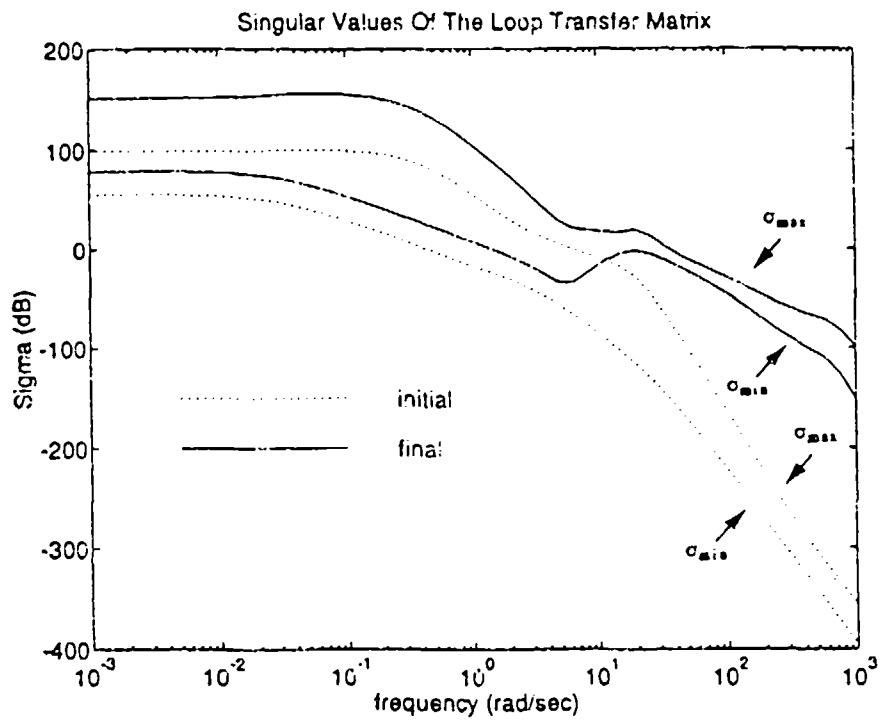
Singular Values Of The Loop Transfer Matrix

Figure 3.3 Loop Transfer Matrices of the Control System

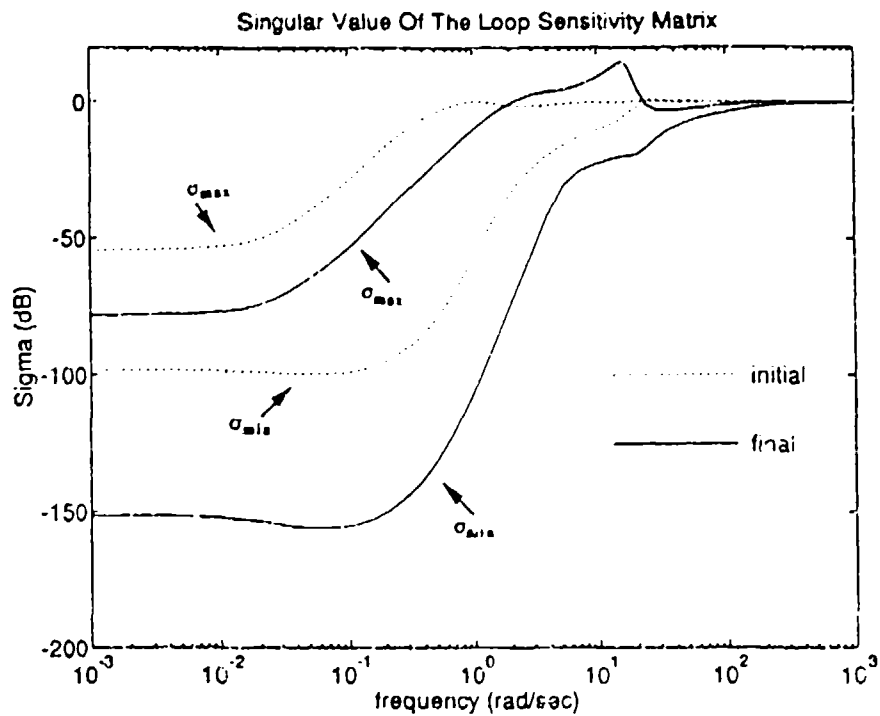Singular Value Of The Loop Sensitivity Matrix

Figure 3.4 Loop Sensitivity Matrices of the Control System

3.4. The Control Analysis And Synthesis Procedure Using μ

Procedures for numerical computations in μ-analysis and μ-synthesis are discussed in view of the analytical results of Section 2 and the simulation results of Section 3. Given a nominal plant, the perturbed parameter and uncertainty structure, the design specifications, and a set of MIMO controllers (that are already designed), the following procedural rules are presented for analysis and comparison of these controllers in view of their nominal and robust stability and performance.

Step 1: Break the loop at selected points according to the uncertainty structure and perturbed parameters;

Step 2: Select the weighting functions for stability and performance according to the design specifications and knowledge of the uncertainty structures;

Step 3: Build the augmented open-loop system structure which includes the nominal plant, and the weighting functions;

Step 4: Use each of the designed controllers to close the loop and construct the augmented M-block for μ-analysis;

Step 5: Check whether each pole of the M-block is located in the left half s-plane. Choose those controllers that are stable.

Step 6: Use the μ-analysis program (MU_ANLY.M described in Section 4) to compare $\|M_{22}\|_\infty$ for each design and choose those controllers that most closely satisfy the nominal performance requirements.

Step 7: Compare $\|\mu(M_{11})\|_\infty$ for each design and choose those controllers that most closely satisfy the robust stability.

Step 8: If the robust performance is the major concern of the design objective, then $\|\mu(M)\|_\infty$ of the candidate controllers should be compared first. Otherwise, use different uncertainty structures and repeat μ-analysis to verify if the robust stability of the controller is sensitive to a change in the uncertainty structure. Choose those controllers that most closely satisfy the robust performance or are relatively less sensitive to changes in the uncertainty structure.

Step 9: Conduct a time domain simulation on the controllers that have passed the above tests for the actual closed-loop system structure under the worst case perturbations. Select those controllers which provide a good performance of the closed-loop system.

4. DESCRIPTION OF THE COMPUTER CODE

A number of programs are written in the MATLAB environment [Moler et al. (1987); Balas et al. (1991)] for robustness analysis with any multivariable plant model and uncertainty blocks. The program MU_EXAMP.M demonstrates the usage of the above programs by analyzing the flight control system of an advanced aircraft. discussed in Chapter 3 and following the program structure shown in Figure 4-1. However, to use these programs in the specific μ-analysis and μ-synthesis problem, the user should write his or her own program.

MU_INIT.M

This program creates an interconnection structure of a given open loop system. It must be run before any controller design and μ-analysis.

Input: A, B, C, D - nominal plant state space matrices.

G_{del} - gain of uncertainty weighting function.

G_p - gain of performance weighting function.

Output: W_{del} - uncertainty weighting function.

W_p - performance weighting function.

p_block - interconnected structure of the open loop system.

Since the interconnection structure is specific for each individual system, the program written inside MU_INIT.M should be changed in each case. The user should know how to build the interconnection structures using the MATLAB function "sysic" [Balas et al. (1991)]. Figure 4-2 gives the interconnection structure used in the example given in Chapter 3. Three different methods, namely, LQG, H_2 and H_∞ for the initial step of controller design are provided in the programs called MU_LQG.M, MU_H2.M and MU_HINF.M, respectively.
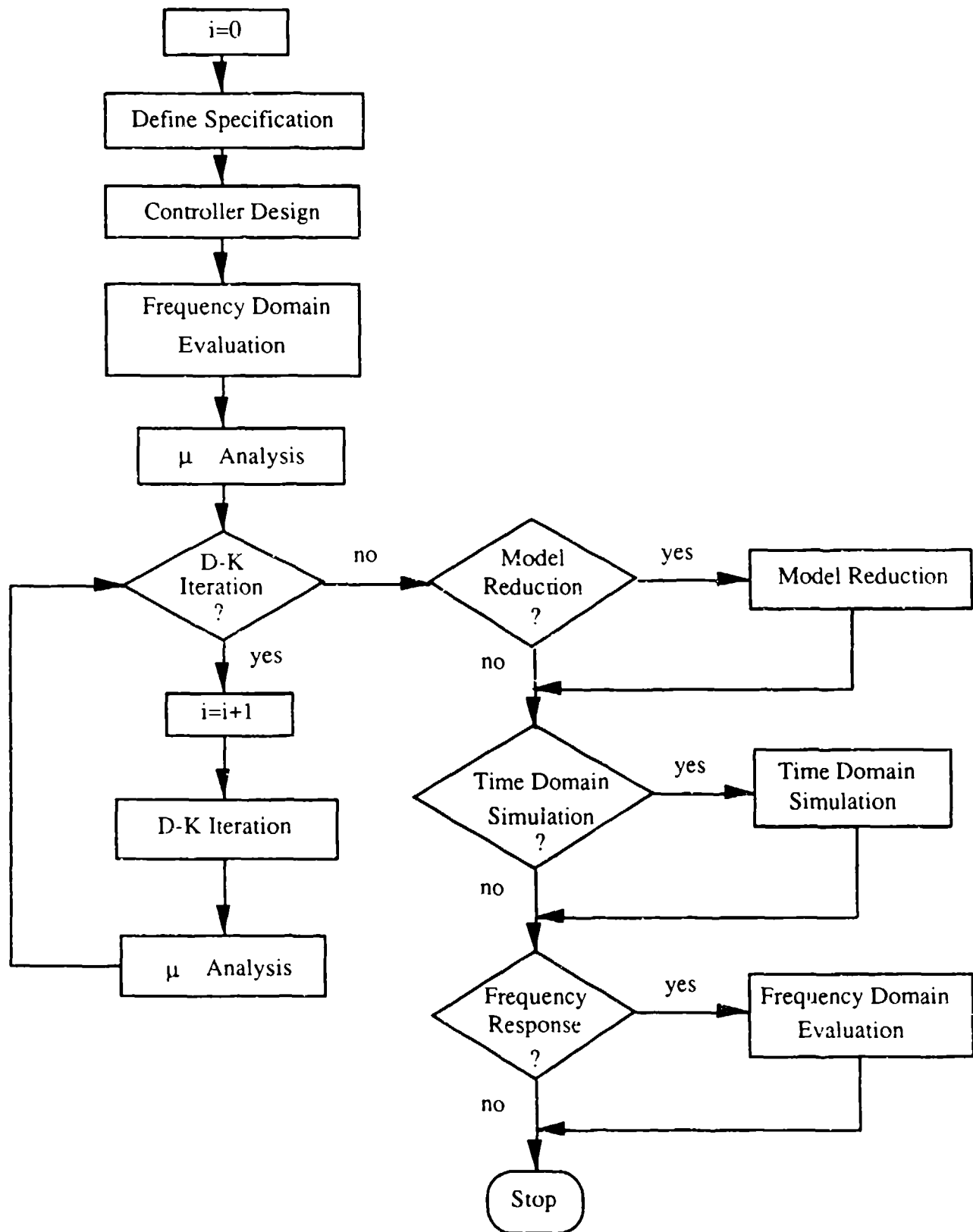
Figure 4-1. Control Systems Analysis and Synthesis Program Flow Chart

MU_LQG.M

This program carries out LQG controller design. It can be used as the initial step of the μ-synthesis.

Input: A, B, C, D - plant state space matrices

          Q_c, R_c - weighting matrices for LQR design

          Q_f, R_f - plant disturbance and measurement error covariance, respectively

Output: F - controller gain

          L - observer gain

          k_comp - compensator structure

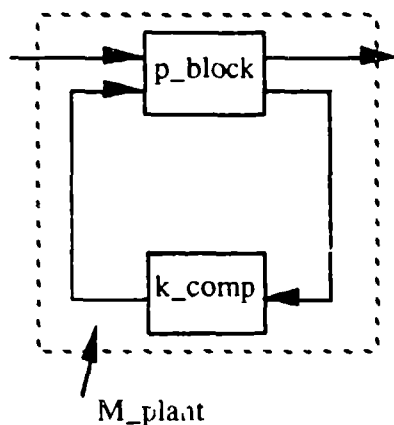   M_plant - closed-loop system structure as shown in Figure 4-2.

Figure 4-2. The Closed-Loop System M_plant.

MU_H2.M

This program carries out H2 controller design. It can be used as the initial step for μ-synthesis.

Input: p_block - open-loop system structure

Output: k_comp - compensator structure

          M_plant - closed-loop system structure

MU_HINF.M

This program does H∞ controller design. It can be used as the initial step for μ-synthesis.

Input: p_block - open-loop system structure

Output: k_comp - compensator structure

M_plant - closed-loop system structure

The next step after controller design and evaluation is μ-analysis as seen in the flow chart of Figure 4-1.
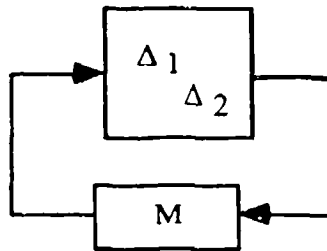

Figure 4-3. The Structure Used in the μ-analysis

MU_ANLY.M

This program carries out μ-analysis.

Input: M_plant - closed-loop system structure

blk1 - block structure of Δ_1 as shown in Figure 4-3.

blk2 - block structure of Δ_2 as shown in Figure 4-3.

blk - block structure of $\Delta = \begin{bmatrix} \Delta_1 & 0 \\ 0 & \Delta_2 \end{bmatrix}$

Output: frequency domain plot of $\bar{\sigma}(M_{22})$, and $\|M_{22}\|_\infty$ as the measure of nominal performance.

frequency domain plot of $\mu(M_{11})$, max($\mu(M_{11})$), and $\|\Delta_1\|_\infty$ as the measure of robust stability

frequency domain plot of $\mu(M)$, max($\mu(M)$), and $\|\Delta\|_\infty$ as the measure of robust performance.

At this stage the user may choose to further improve the controller via the D-K algorithm of μ-synthesis or directly examine the performance of controller via time-domain simulation.

Note: When typing the input of blk1, blk2, and blk from the keyboard, it is required to use the same format as prescribed in [Balas et al. (1991) pp. 4-70].

MU_DK.M

This program dose D-K iteration as a part of μ-synthesis.

Input: p_block - original open-loop system structure

rpdvec - D matrices obtained by μ-analysis

rpsens - sensitivity function of $\mu(\cdot)$ obtained by μ-analysis

blk - block structure of $\Delta = \begin{bmatrix} \Delta_1 & 0 \\ 0 & \Delta_2 \end{bmatrix}$

Output: k_comp - compensator structure with increased order during the iteration. This is designed according to the new open loop system structure shown in Figure 4-4.

M_plant - closed-loop system structure with increased order during the iteration.
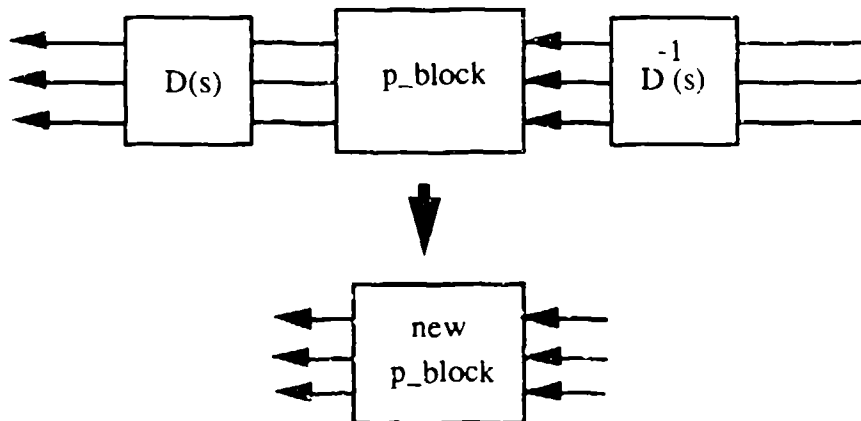

Figure 4-4. Augmention via D-Matrices in the D-K Iteration

28

MU_SIMU.M

This program does time domain simulation of the closed loop system with the worst perturbation as a stable transfer matrix.

Input: M_plant1 - closed-loop system structure of the initial design

in_pvec - perturbations of the initial design obtained from μ-analysis

in_bnds - upper and lower μ bounds of the initial design obtained from μ-analysis

M_plant2 - closed-loop system structure of the final design

fin_pvec - perturbations of the final design obtained from μ-analysis

fin_bnds - upper and lower μ bounds of the final design obtained from μ-analysis

n_block - number of blocks to be approximated by transfer matrix

blk - block structure of $\Delta = \begin{bmatrix} \Delta_1 & 0 \\ 0 & \Delta_2 \end{bmatrix}$

Output: M_pert1 - closed-loop system structure of the initial design with the worst perturbation as shown in Figure 4-5.

M_pert2 - closed-loop system structure of the final design with the worst perturbation

u - time domain input signal

y1 - output signal of the initial design

y2 - output signal of the final design
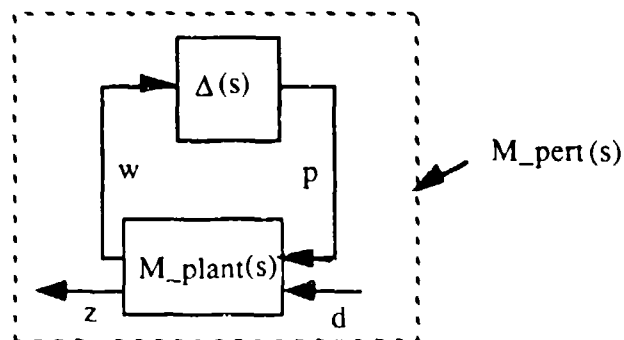
Figure 4-5. Closed-Loop System with the Worst-Case Perturbation

MU_FRQ.M

This program plots singular values of loop transfer matrices and sensitivity matrices for a closed-loop system.

Input: ap,bp,cp,dp - plant state space matrices

ak,bk,ck,dk - compensator state space matrices

ak2,bk2,ck2,dk2 - second compensator state space matrices

n_comp - number of closed-loop systems. If n_comp=1, then only one loop is plotted; if n_comp =2, then two loop functions are plotted in one graph.

Output: sx1 - singular values of the loop transfer matrices

sy1 - singular values of the loop sensitivity matrices

sx2 - singular values of the second loop transfer matrices, if n_comp=2

sy1 - singular values of the loop sensitivity matrices, if n_comp=2

5. SUMMARY AND CONCLUSIONS

This report presents the results of control systems analysis and their applications to control systems synthesis for high performance aircraft, and provides a proven, tractable and portable methodology to quantify the stability margins and robustness of highly integrated digital fly-by-wire control systems. The H_∞–based μ–analysis approach has been recommended for quantitative evaluation of robust stability and performance of multi-input multi-output (MIMO) control systems. This approach for control systems evaluation offers an alternative to the notions of conventional gain margin and phase margin.

A survey of recent literature has shown three major different approaches to quantitatively evaluate the robust stability and performance of MIMO control systems. The first approach relies on the structured singular value (μ) and H_∞–analyses in the framework of Linear Fractional Transformations (LFT) of MIMO systems that are subjected to uncertainties with known bounds. The second approach generalizes the definition and calculation of gain and phase margins for MIMO systems analogous to those for single-input, single-output (SISO) systems. The third approach examines the relationships between the open loop gain and phase with respect to closed loc, sitivity and complementary sensitivity functions for SISO systems, and then formulates heuristic rules for shaping the loop transfer functions for MIMO systems. The first approach of μ-analysis for robustness assessment of MIMO systems constitutes the main body of this report because it has significant advantages over the remaining two approaches as discussed below.

The second approach attempts to generalize the conventional concepts and computation algorithms of gain margin and phase margin for MIMO systems. The concepts of gain margin and phase margin were initially based on gain parameter perturbations of a given controller for SISO closed-loop systems. The algorithm, generalized for MIMO systems in the second approach, can only deal with parameter variations of a constant gain matrix. Since a MIMO plant is generally represented by a stabilizable, real-rational transfer matrix, the system gain margin is not uniquely defined. Therefore, analysis of MIMO control systems based on gain margin and phase margin is not a straight-forward extrapolation of that of SISO systems. In contrast, the concept of structured singular value (μ) deals with all types of bounded parametric and non-parametric uncertainties. Apparently μ-analysis appears to be much more general than any of the reported algorithms for gain margin and phase margin evaluation. The μ-analysis can handle not only the parameter variations in the dynamic controller $K(s)$ but also the uncertainties in the plant model and parameter perturbations anywhere in the loop. To summarize, μ-analysis is capable of quantifying the stability and robustness of the closed-loop system under any destabilizing factor. Furthermore, the algorithms in the second approach are relatively more conservative because singular values of

the transfer matrices are often used as the norm to bound the perturbations, and the parameters are only allowed to vary diagonally. In contrast, μ-analysis does not suffer from these problems because the notion of structured singular value is directly based on the Nyquist stability theorem.

Although the third approach which is based on loop transfer matrices is more general than the second approach for MIMO control systems, it only provides a qualitative description of the stability and performance of closed-loop systems. Apparently, quantitative analysis of stability and performance can be reliably carried out by the algorithms based on μ. Therefore, μ-analysis is considered to be the most effective tool for control systems evaluation as reported in open literature.

Results of simulation experiments using the flight dynamic model of an advanced aircraft have been presented to demonstrate how the nominal and robust stability and performance can be evaluated via μ-analysis. Furthermore, it is shown that both stability and robustness can be improved using the tools of μ-synthesis. A software package has been developed in the environment of MATLAB for analyzing robustness of MIMO control systems. This package is built upon the commercially available μ-Analysis and Synthesis Toolbox [Balas et al. (1991)].

APPENDIX A

THE PRINCIPLE OF MULTIVARIABLE NYQUIST STABILITY CRITERION

Let $N(A, f(s), C)$ denote the number of clockwise encirclements of the point A in the complex plane by the image of the clockwise contour C under the mapping $f(s)$. Using this notation, the principle of the argument can be written as:

$$N(0, f(s), C) = Z - P$$

where Z is the number of zeros of $f(s)$ inside C, and P is the number of poles of $f(s)$ inside C.

Suppose $f(s) = f_1(s)f_2(s)$ and there are no pole-zero cancellations between $f_1(s)$ and $f_2(s)$. Then, the Nyquist stability criterion is stated as follows:

$$N(0, f_1(s)f_2(s), C) = N(0, f_1(s), C) + N(0, f_2(s), C)$$

Proof of the Nyquist Stability Criterion:

Let the contour D_R enclose right half plane. The closed loop system is stable if and only if

$$N(0, \Phi_{cl}(s), D_R) = 0$$

Therefore, $N(0, \Phi_{ol}(s)det(I + G(s)), D_R) = N(0, \Phi_{ol}(s), D_R) + N(0, det(I + G(s)), D_R) = 0$.

Let $P_{u,ol}$ denote the number of unstable open-loop poles of $G(s)$. Then

$$N(0, \Phi_{ol}(s), D_R) = P_{u,ol} \text{ and } N(0, det(I + G(s)), D_R) = -P_{u,ol} \qquad \blacklozenge$$
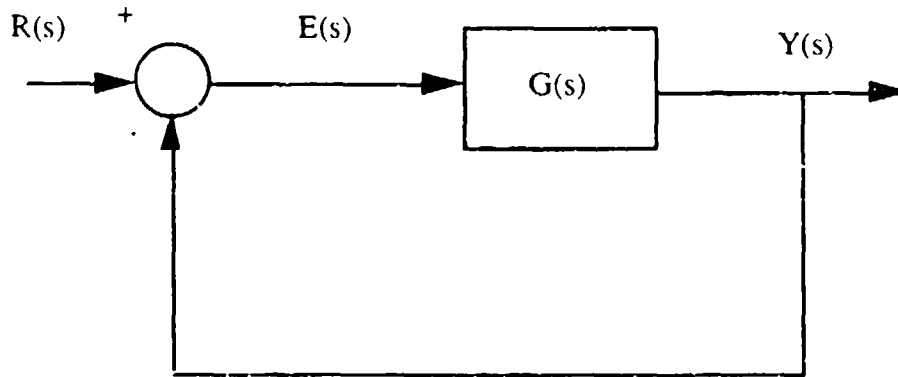

Figure A-1. Multivariable Feedback System

Given the plant in Figure A-1, the relationship between the open loop and closed loop characteristic polynomials is as follows [Desoer et al. (1977)]:

$$\Phi_{cl} = \Phi_{ol} \, det[I + G(s)] \qquad\qquad\qquad (A\text{-}1)$$

or $\qquad \Phi_{cl} = det[sI - A_{cl}] \qquad\qquad\qquad\qquad (A\text{-}2)$

where $\Phi_{ol} = det[sI - A]$ is the open loop characteristic polynomial, A and A_{cl} are the system matrices of the open loop system, $G(s)$, and the closed loop system, $G(s)[I + G(s)]^{-1}$, respectively.

The Nyquist stability criterion states that the closed-loop system is stable if and only if the number of counter-clockwise encirclements of the origin by the image of the clockwise Nyquist contour D_R under the mapping $det(I + G(s))$ equals the number of unstable open-loop poles of the open-loop transfer matrix $G(s)$. The proof of this criterion is based on the theory of complex analysis as outlined earlier in this Appendix. Several researchers [Yeh et al. (1985a), Molander and Willems (1980), Tao et al. (1991), Lehtomaki et al. (1981)] have attempted to extend the concepts of gain and phase margins of SISO systems to address the stability robustness of MIMO systems.

APPENDIX B
APPROACH 2: MULTIVARIABLE GAIN MARGIN AND PHASE MARGIN

Now we introduce the pertinent definitions and some of the useful algorithms for the aforementioned two approaches of robustness assessment.

Some diversity and ambiguity exist in defining the MIMO gain and phase margins. The common practice of one-loop-at-a-time stability margins fails to account for the simultaneous variations in MIMO feedback systems and hence may not be acceptable as relative stability measures. The norm-bounded robustness criteria guarantee closed-loop stability but they do not explain how the individual elements of the control gain matrix may be varied without destabilizing the closed-loop system. To this effect, Yeh et al (1985a) introduced two different definitions of stability margins.

Definition B-1: independent gain margins are limits within which the gains of all feedback loops may be varied simultaneously and independently without destabilizing the system while the phase angles remain at their nominal values. Independent phase margins are limits within which the phase angles of all feedback loops may be varied simultaneously and independently without destabilizing the system while the gains of all feedback loops remain at their nominal values. However, these stability margins, if computed via the singular-value based robust stability criteria, tend to be very conservative.

Definition B-2: Uniform gain margins are limits within which the gains of all feedback loops may be varied uniformly without destabilizing the feedback system while the phase angles remain at their nominal values. Uniform phase margins are limits within which the phase angles of all feedback loops may be varied uniformly without destabilizing the system while the gains remain at their nominal values.

Remark:: A major difference between MIMO and SISO systems is that the stability margins of MIMO systems vary relative to the point where the complex loop gains are measured. For a general feedback system, if the gain perturbations are calculated at input of the plant, then the simultaneous perturbation in each loop may be represented by a diagonal perturbation matrix $L(s)$ preceding the plant $G(s)$.

For independent margins: $\quad L(j\omega) = diag[b_1(\omega)e^{jq_1(\omega)}, b_2(\omega)e^{jq_2(\omega)}, ..., b_n e^{jq_n(\omega)}]$ $\quad$ (B-1)

For uniform margins: $\quad L(j\omega) = \beta(\omega)e^{j\theta(\omega)}I$ $\hfill$ (B-2)

There are several different ways to calculate the stability margins [Yeh et al. (1985a), Molander and Willems (1980), Tao et al. (1991)]. However, we discuss the following three algorithms in this report.

<u>Robustness Bound For Perturbation Errors</u>: [Yeh et al. (1985a)]

Let $G(s)$ and $\tilde{G}(s)$ represent the nominal and perturbed open-loop transfer matrices, respectively, and the multiplicative and inverse multiplicative perturbations are given as follows:

$$E(s) = \begin{cases} [\tilde{G}(s) - G(s)]G^{-1}(s) & \text{for multiplicative perturbations} \\ [\tilde{G}^{-1}(s) - G^{-1}(s)]G(s) & \text{for inverse multiplicative perturbations} \end{cases} \tag{B-3}$$

In eqs. (B-1) and (B-2), the gain and phase perturbations $L(s) = E(s) + I$. The singular value based robustness tests are given as follows [Lehtomaki et al. (1981)]:

$$\overline{\sigma}[L - I] < \underline{\sigma}[I + G^{-1}] \quad \text{for multiplicative perturbation, and} \tag{B-4}$$

$$\overline{\sigma}[L^{-1} - I] < \alpha < \underline{\sigma}[I + G], \quad \alpha \leq 1 \quad \text{for inverse multiplicative perturbation.} \tag{B-5}$$

It has been shown [Yeh et al. (1985b)] by using the inverse Nyquist criterion and the Nyquist criterion that the robustness tests for (B-3) are:

$$\overset{max}{\underset{i}{}}|\lambda_i[L - I]| < \overset{min}{\underset{i}{}}|\lambda_i[I + G^{-1}]| \quad \text{for multiplicative perturbation, and} \tag{B-6}$$

$$\overset{max}{\underset{i}{}}|\lambda_i[L^{-1} - I]| < \alpha \leq \overset{min}{\underset{i}{}}|\lambda_i[I + G]|, \quad 0 \leq \alpha \leq 1$$

$$\text{for inverse multiplicative perturbation.} \tag{B-7}$$

The independent gain margin (IGM) is obtained by substituting (B-2) into (B-4) and then letting the phase angles $\theta_1 = \theta_2 = \cdots = \theta_n = 0$, and $a_1 = \underline{\sigma}[I + G^{-1}]$

$$1 - a_1 < \beta_i(\omega) < 1 + a_1 \qquad \forall i \tag{B-8}$$

Letting the gains $\beta_1 = \beta_2 = \cdots = \beta_n = 1$, the independent phase margin (IPM) is obtained as:

$$-2\sin^{-1}(a_1/2) < \theta_i(\omega) < 2\sin^{-1}(a_1/2) \qquad \forall i, \quad a_1 \leq 2 \tag{B-9}$$

$$\text{and} \quad -\pi < \theta_i(\omega) < \pi \qquad \forall i, \quad a_1 > 2 \tag{B-10}$$

36

Similarly, substituting (B-3) into (B-5) and the IGM and IPM for inverse multiplicative perturbations are obtained as:

$$\frac{1}{1+\alpha_1} < \beta_i(\omega) < \frac{1}{1-\alpha_1} \qquad \forall i \qquad \text{where } \alpha_1 = \underline{\sigma}[I+G], \text{ and} \qquad \text{(B-11)}$$

and $\qquad -2\sin^{-1}(\alpha_1/2) < \theta_i(\omega) < 2\sin^{-1}(\alpha_1/2) \qquad \forall i \qquad$ (B-12)

Substituting (B-3) into (B-6) and (B-7), the uniform gain margin (UGM) and uniform phase margin (UPM) can be obtained as:

For multiplicative perturbation: $a_0 = \underset{i}{min} \left| \lambda_i \left[I + G^{-1} \right] \right|$ under the following constraints:

$$1 - a_0 < \beta(\omega) < 1 + a_0 \qquad \text{(B-13)}$$

$$-2\sin^{-1}(a_0/2) < \theta(\omega) < 2\sin^{-1}(a_0/2) \qquad a_0 \leq 2 \qquad \text{(B-14)}$$

$$-\pi < \theta(\omega) < \pi \qquad a_0 > 2 \qquad \text{(B-15)}$$

For inverse multiplicative perturbation: $\alpha_0 = \underset{i}{min} \left| \lambda_i [I+G] \right|$ under the following constraints:

$$\frac{1}{1+\alpha_0} < \beta(\omega) < \frac{1}{1-\alpha_0} \qquad , \qquad \text{(B-16)}$$

$$-2\sin^{-1}(\alpha_0/2) < \theta(\omega) < 2\sin^{-1}(\alpha_0/2) \qquad \text{(B-17)}$$

The advantages of using this algorithm to calculate MIMO gain margins and phase margins are that relatively simple formulae can be derived from the robustness bound concepts. Although the independent gain and phase margins are rather conservatively based on singular values, the combined use of IGM, IPM, UGM and UPM yields a less conservative estimate of the stability perturbing region in the gain space and phase space [Yeh et al. (1984)]. However, the major disadvantage is that these perturbations are only constrained at diagonal elements of the perturbation matrix There is apparently no discussion about the off-diagonal terms.

<u>Perturbation With Nonlinear Cone Boundary</u> [Molander and Willems (1980)]

For MIMO linear-quadratic regulators, there is Kalman's inequality which implies that this kind of controllers possess a 60° phase margin, infinite gain margin, and 50 percent gain reduction tolerance [Safonov and Athans (1977)]. Using this result, Molander and Willems (1980)

developed a procedure for synthesizing state feedback control of multivariable systems with specified gain and phase margins. Considering the linear time-invariant finite-dimensional systems:

$$\dot{x} = Ax + Bu \tag{B-18}$$

with $x \in R^n$, $u \in R^m$, and the pair (A, B) being controllable, and the desired input being given by the linear time-invariant state feedback control law:

$$u = -L^T x \tag{B-19}$$

The above equation (B-19) is called a robust control law with robustness sector (K_1, K_2) with $-\infty \le K_1 \le 1 \le K_2 \le \infty$ if the closed-loop system is globally asymptotically stable. The sector condition is illustrated in Figure B-1 for the single-input case. The control input is given by

$$u = -f(L^T x, t) \tag{B-20}$$

with $f : R^m \times R \to R^m$ being any nonlinear function satisfying the following condition:

$$\sup_{\sigma, t} (f(\sigma, t) - K_1 \sigma)^T (f(\sigma, t) - K_2 \sigma) < 0 \tag{B-21}$$

Or, equivalently, $\displaystyle \sup_{\sigma, t} \frac{\left| f(\sigma, t) - 1/2(K_1 + K_2)\sigma \right|}{|\sigma|} < \frac{1}{2}(K_2 - K_1)$ \hfill (B-22)
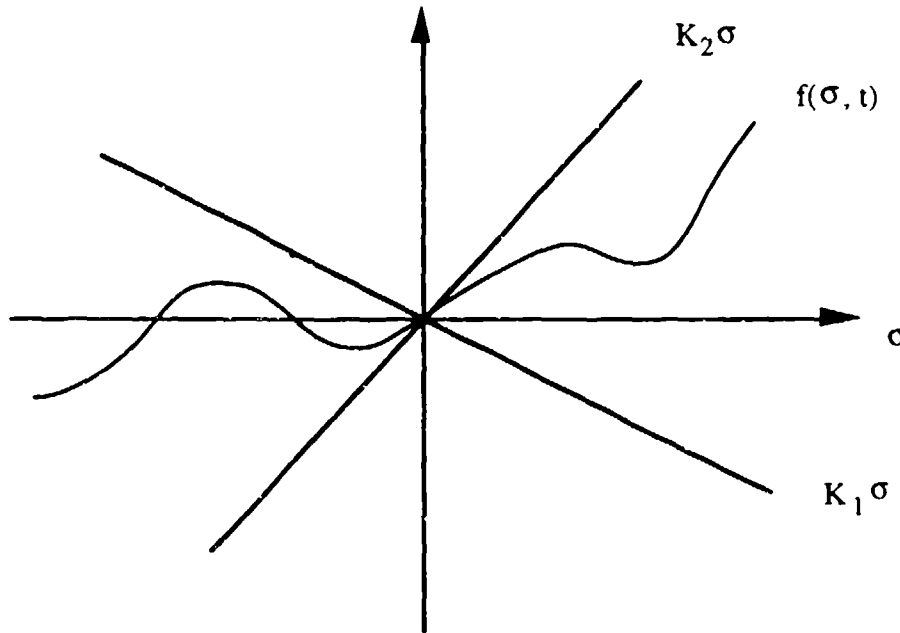

Figure B-1. An Illustration of the Sector Condition

The robustness requirements also allow for an interpretation in terms of gain and phase margins and gain reduction tolerance (defined below). The control law (B-19) has a gain margin g ($g \geq 1$) if the closed-loop system is globally asymptotically stable for all control laws:

$$u = -\Lambda L^T x \qquad (B-23)$$

where Λ is any symmetric matrix with eigenvalues $1 \leq \lambda_i \leq g$. The system is said to have a phase margin ϕ ($0 \leq \phi \leq \pi$) if it is globally asymptotically stable for all control laws (B-23) with Λ being any unitary matrix possessing eigenvalues $\lambda_i = exp(j\phi_i)$ with $|\phi_i| \leq \phi$. It is said to have a gain reduction tolerance ρ if it is globally asymptotically stable for all control laws (B-23) with Λ any symmetric matrix with eigenvalues $(1 - \rho) \leq \lambda_i \leq 1$. The relationship between robustness sector (K_1, K_2) and the gain and phase margins are:

$$g = K_2 \qquad (B-24)$$

$$\rho = (1 - K_1) \times 100 \qquad (B-25)$$

$$cos(\phi) = \frac{K_1 K_2 + 1}{K_1 + K_2} \qquad (B-26)$$

Using the multivariable control system stability theory, a methodology has been developed [Molander and Willems (1980)] to synthesize the linear quadratic control law under prescribed gain and phase margins. A similar synthesis procedure has been developed for the discrete-time state feedback control law by [Lee and Lee (1986)].

The advantages of the above control algorithm are that the synthesis is based on the framework of the general state feedback control law, which can be directly obtained with a given robustness sector by solving the matrix Riccati equation. The major disadvantage of this algorithm is that it is apparently restricted to the full-state feedback control case and does not address the general compensator structures.

Unity-Feedback Multivariable Control System [Tao et al. (1991)]

In this method, the boundaries of gain and phase margins of multivariable control systems are obtained by decomposition into augmented open-loop transfer functions. Then the characteristic equations are formulated and the stability margins are tested. Consider the multivariable feedback control systems shown in Figure B-2.
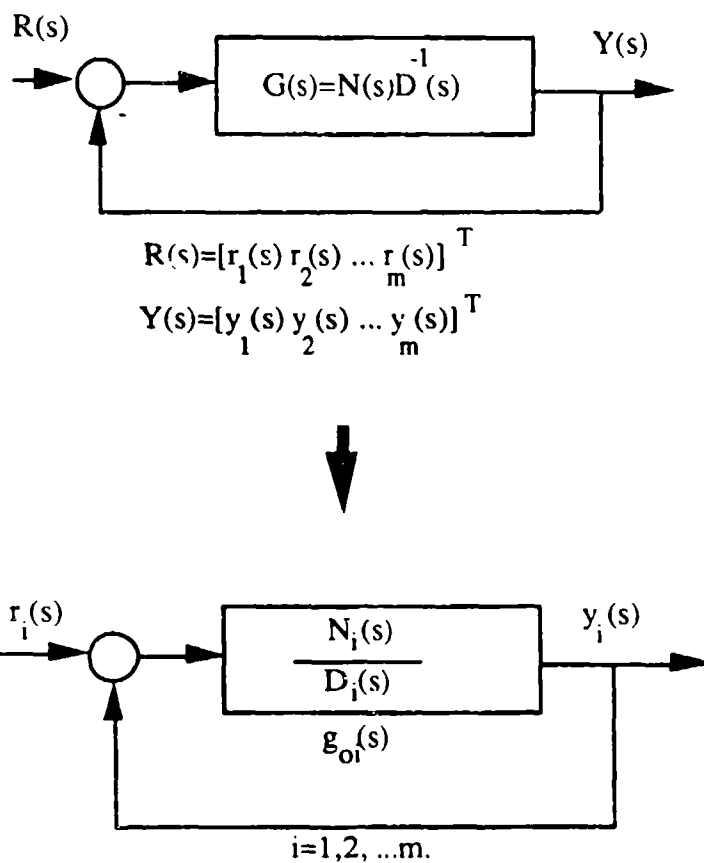
Figure B-2. Multivariable System Represented by Augmented Open-Loop Transfer Function

The proper transfer function $G(s)$ is:

$$G(s) = \begin{bmatrix} G_{11} & G_{12} & \dots & G_{1i} & \dots & G_{1m} \\ G_{21} & G_{22} & & G_{2i} & & G_{2m} \\ \vdots & \vdots & & \vdots & & \vdots \\ G_{i1} & G_{i2} & \dots & G_{ii} & \dots & G_{im} \\ \vdots & \vdots & & \vdots & & \vdots \\ G_{m1} & G_{m2} & \dots & G_{mi} & \dots & G_{mn} \end{bmatrix} = N(s)D^{-1}(s)$$

(B-27)

where the relatively coprime polynomial matrices, $N(s)$ and $D(s)$, are expressed as:

$$N(s) = \begin{bmatrix} n_{11} & n_{12} & \cdots & n_{1i} & \cdots & n_{1m} \\ n_{21} & n_{22} & & n_{2i} & & n_{2m} \\ \vdots & \vdots & & \vdots & & \vdots \\ n_{i1} & n_{i2} & \cdots & n_{ii} & \cdots & n_{im} \\ \vdots & \vdots & & \vdots & & \vdots \\ n_{m1} & n_{m2} & \cdots & n_{mi} & \cdots & n_{mn} \end{bmatrix}$$

(B-28)

and

$$D(s) = \begin{bmatrix} d_{c1} & 0 & \cdots & 0 & \cdots & 0 \\ 0 & d_{c2} & & 0 & & 0 \\ \vdots & \vdots & & \vdots & & \vdots \\ 0 & 0 & \cdots & d_{ci} & \cdots & 0 \\ \vdots & \vdots & & \vdots & & \vdots \\ 0 & 0 & \cdots & 0 & \cdots & d_{cn} \end{bmatrix}$$

(B-29)

The characteristic equation of the closed loop system is

$$det[D(s) + N(s)] = det \begin{bmatrix} d_{c1} + n_{11} & n_{12} & \cdots & n_{1i} & \cdots & n_{1m} \\ n_{21} & d_{c2} + n_{22} & & n_{2i} & & n_{2m} \\ \vdots & \vdots & & \vdots & & \vdots \\ n_{i1} & n_{i2} & \cdots & d_{ci} + n_{ii} & \cdots & n_{im} \\ \vdots & \vdots & & \vdots & & \vdots \\ n_{m1} & n_{m2} & \cdots & n_{mi} & \cdots & d_{cn} + n_{mm} \end{bmatrix} = 0$$

(B-30)

Applying the determinant property [Kreyszig (1972)], eq. (B-30) can be decomposed into the following m different expressions

$$det[D(s) + N(s)] = det[D_{0i}(s)] + det[N_{0i}(s)] = 0, \quad i = 1, 2, \ldots, m$$

(B-31)

where $det[N_{0i}(s)]$ and $det[D_{0i}(s)]$ are defined as:

$$det[N_{0i}(s)] = det \begin{bmatrix} d_{c1} + n_{11} & n_{12} & \cdots & n_{1i} & \cdots & n_{1m} \\ n_{21} & d_{c2} + n_{22} & & n_{2i} & & n_{2m} \\ \vdots & \vdots & & \vdots & & \vdots \\ n_{i1} & n_{i2} & \cdots & n_{ii} & \cdots & n_{im} \\ \vdots & \vdots & & \vdots & & \vdots \\ n_{m1} & n_{m2} & \cdots & n_{mi} & \cdots & d_{cn} + n_{mm} \end{bmatrix} = 0$$

(B-32)

$$det[D_{0i}(s)] = det \begin{bmatrix} d_{c1} + n_{11} & n_{12} & \cdots & 0 & \cdots & n_{1m} \\ n_{21} & d_{c2} + n_{22} & & 0 & & n_{2m} \\ \vdots & \vdots & & \vdots & & \vdots \\ n_{i1} & n_{i2} & \cdots & d_{ci} & \cdots & n_{im} \\ \vdots & \vdots & & \vdots & & \vdots \\ n_{m1} & n_{m2} & \cdots & 0 & \cdots & d_{cn} + n_{mm} \end{bmatrix} = 0$$

(B-33)

Now the augmented open-loop transfer function (AOLTF) is defined as:

$$g_{0i}(s) = \frac{det[N_{0i}(s)]}{det[D_{0i}(s)]} = \frac{N_i(s)}{D_i(s)}$$

(B-34)

For a unity-feedback $m \times m$ multivariable system, there are m AOLTFs. Each of the $g_{0i}(s)$ is a transfer function of $y_i(s)/r_i(s)$ effected by the ith (open) unity-feedback loop, and can be considered as an open-loop transfer function of an unit feedback control system shown in Figure B-2. The gain and phase margins of an unity-feedback multivariable control system are, in fact, the gain margins (GM) and phase margins (PM) of all AOLTFs. For an $m \times m$ unity-feedback multivariable control system, there are m sets of gain margins and phase margins. The calculation of each set is based upon the corresponding AOLTF and can be checked by Nyquist plots.

The advantage of the above synthesis algorithm is that the plotting methods used in SISO feedback loop stability tests can be used directly and therefore the gain and phase margins of each AOLTF are easily formulated. The relationship of the stability margins of AOLTF with parameter perturbations of the original system is discussed by Tao, Cheng and Han (1991). These parameters could be the original system gain perturbations. However, further work is needed is to find the direct relationships of the stability margins of AOLTFs with the original control system.

Each of the above three algorithms is aimed at calculation of the MIMO gain and phase margins analogous to those of SISO systems. However, the ultimate goal is to shape the closed-loop functions such that it satisfies the performance and stability robustness requirements. Since there is a direct relationship between the open loop gain and phase and closed-loop characteristics for SISO systems, the gain margin and phase margin are two parameters to be adjusted to shape the closed-loop transfer function. There could be other parameters to adjust the closed loop transfer functions for MIMO systems. Following this concept, Freudenburg and Looze (1988) have investigated the MIMO closed-loop system properties, and developed rules for shaping the closed-loop sensitivity function and complementary sensitivity function by adjusting the open loop gain, phase and directions.

APPENDIX C

APPROACH 3: MULTIVARIABLE LOOP SHAPING

Classical "loop-shaping" design methods proceed directly with manipulation of open loop gain and phase to alter the feedback properties of the system [Freudenburg and Looze (1986), Freudenburg (1990), Freudenburg and Looze (1988)]. Clearly, one reason for the success of these methods is that, for a SISO system, open loop gain and phase can be readily related to the feedback properties. The loop transfer function $L(j\omega)$ has the following properties:

$$|L(j\omega)| \gg 1 \Leftrightarrow \begin{array}{l} |S(j\omega)| \ll 1 \\ and \\ T(j\omega) \approx 1 \end{array} \tag{C-1}$$

and

$$|L(j\omega)| \ll 1 \Leftrightarrow \begin{array}{l} |T(j\omega)| \ll 1 \\ and \\ S(j\omega) \approx 1 \end{array} \tag{C-2}$$

At frequencies for which the open loop gain is approximately unity, feedback properties depend critically upon the open loop phase:

$$\begin{array}{l} |L(j\omega)| \approx 1 \\ and \\ \angle L(j\omega) \approx \pm 180^0 \end{array} \Leftrightarrow \begin{array}{l} |S(j\omega)| \gg 1 \\ and \\ |T(j\omega)| \gg 1 \end{array} \tag{C-3}$$

Heuristic rules used in design: First, large loop gain yields small sensitivity and good disturbance rejection properties, although noise appears directly in the system output. Second small loop gain is required for small noise response and for robustness against large multiplicative uncertainty. Finally, at frequencies near gain crossover (i.e., $|L(j\omega)| = 1$), phase of the open loop system must remain bounded sufficiently far away from $\pm 180^0$ to provide an adequate stability margin and to prevent amplifying the disturbances and noise.

Generalization of Scalar Concepts to Multivariable Systems

Under certain conditions, multivariable systems behave sufficiently like SISO systems such that classical results can be easily extended. First, it is assumed that the plant to be controlled has a well-conditioned transfer function matrix. It is also necessary to assume that the disturbances are injected into the system at the same loop-breaking point at which uncertainties exist, and that the

levels of uncertainty, noise, and disturbances are approximately equal in all loops of the system. Hence, the disturbance and noise signals should satisfy the following conditions of upper bound:

$$\|d(j\omega)\| \leq M_d(\omega) \qquad \forall \omega \text{ and}$$

$$\|n(j\omega)\| \leq M_n(\omega) \qquad \forall \omega \tag{C-4}$$

where $M_x(\omega)$ is an upper bound of the norm of a given transfer matrix $x(j\omega)$.

We assume that: (i) each of the outputs of the system is significant; and (ii) the response of each to disturbances and noise is desired to be small. Therefore, the following assumptions need to satisfied:

$$\|y_d(j\omega)\| \leq M_{y_d}(\omega) \quad \forall \omega \text{ and}$$

$$\|y_n(j\omega)\| \leq M_{y_n}(\omega) \quad \forall \omega \tag{C-5}$$

The above assumptions imply that design specifications can be translated into the bounds:

$$\overline{\sigma}[S_o(j\omega)] \leq M_s(\omega), \qquad \forall \omega \text{ and} \tag{C-6}$$

$$\overline{\sigma}[S_o(j\omega)] \leq M_s(\omega), \qquad \forall \omega \tag{C-7}$$

Since there is a conflict between achieving these two goals at the same frequency:

$$S_o(s) + T_o(s) = I \tag{C-8}$$

there is a trade-off between the feedback properties governed by S_o and those governed by . The lack of directionality properties and structure in the systems implies that this trade-off is essentially the same as that in the SISO case. In special cases, the heuristic rules relating the open loop gain to feedback properties can be extended to MIMO systems. Let $L(j\omega) \in C^{n \times n}$ be a transfer function evaluated at a given frequency ω. The level of gain experienced by an input to the system described by this transfer function will generally depend upon the direction in which the input lies. Using the singular value decomposition:

$$L = \sum_{i=1}^{n} v_i u_i^H \sigma_i \tag{C-9}$$

If the open loop transfer matrix has large gains in all directions or small gains in all directions, the following analogs to (C-1) and (C-2) are useful in assessing the feedback properties of the system:

$$\underline{\sigma}[L_o(j\omega)] \gg 1 \Leftrightarrow \begin{array}{c} \overline{\sigma}[S_o(j\omega)] \ll 1 \\ \text{and} \\ T_o(j\omega) \approx I \end{array} \tag{C-10}$$

and

$$\overline{\sigma}[L_o(j\omega)] \ll 1 \Leftrightarrow \begin{array}{c} \overline{\sigma}[T_o(j\omega)] \ll 1 \\ \text{and} \\ S_o(j\omega) \approx I \end{array} \tag{C-11}$$

Multivariable Design Specifications

Suppose that sensors in some loops of the system have become noisy at a lower frequency than the sensors in the other loops. This situation can be mathematically modeled by assuming that the sensor noise can be written as the sum of a structured and an unstructured component:

$$n(s) = n_s(s) + n_u(s) \tag{C-12}$$

The structured noise n_s is assumed to lie in a k-dimensional subspace $N_s \subseteq C^n$, and satisfies the following bound:

$$\|n_s(j\omega)\| \le M_{n_s}(\omega), \quad \forall \omega \tag{C-13}$$

The remaining unstructured component of the noise satisfies the bound:

$$\|n_u(j\omega)\| \le M_{n_u}(\omega) \quad \forall \omega \tag{C-14}$$

Suppose that the ratios $M_{n_s}(\omega) / M_d(\omega)$ and $M_{n_u}(\omega) / M_d(\omega)$ are as depicted in Figure C-1. Let the orthogonal projections onto N_s, the subspace which contain the structured noise, and onto $N_s^\perp$, its orthogonal complement, be denoted by P_s and $P_s^\perp$, respectively. Then the design specifications for this system should satisfy the following conditions:

$$\overline{\sigma}[S_o(j\omega)] \ll 1 \qquad \omega \le \omega_1 \tag{C-15}$$

$$\overline{\sigma}[T_o(j\omega)P_s] \ll 1 \qquad \omega \ge \omega_2 \tag{C-16}$$

$$\overline{\sigma}[S_o(j\omega)P_s^\perp] \ll 1 \qquad \omega \le \omega_3 \tag{C-17}$$

$$\overline{\sigma}[T_o(j\omega)] \ll 1 \qquad \omega \ge \omega_4 \tag{C-18}$$

$$\overline{\sigma}[S_o(j\omega)] \le M_S(\omega) \quad \forall \omega \tag{C-19}$$

$$\overline{\sigma}[T_o(j\omega)] \le M_T(\omega) \quad \forall \omega \tag{C-20}$$
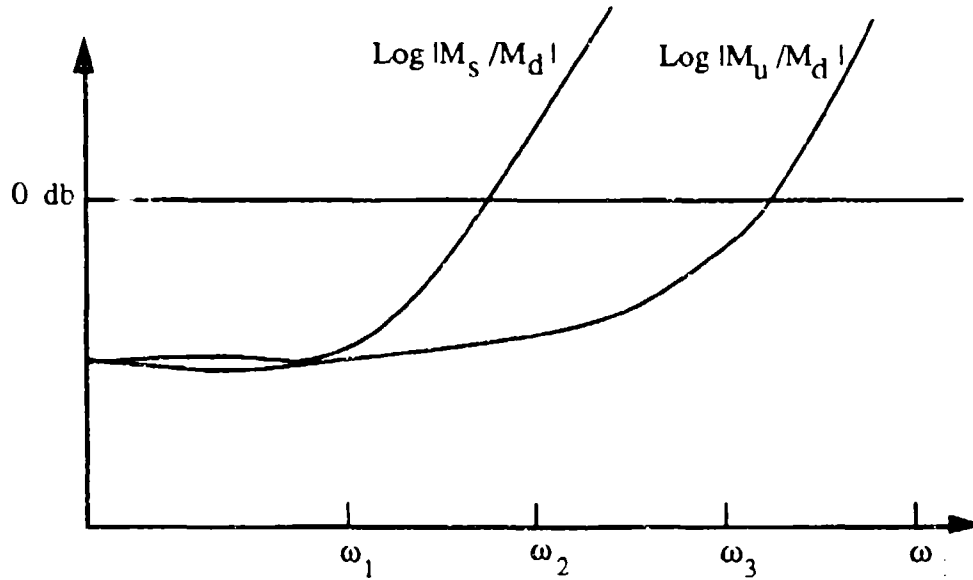
Figure C-1. Relative Levels of Sensor Noise to Disturbance Inputs.

The above specifications could be satisfied by requiring the loop gain to be large in the directions for which the sensitivity is required to be small, and small in the directions for which the complementary sensitivity is required to be small. To describe the gain in different directions, the singular value decomposition of the loop transfer matrix L is partitioned as:

$$L = V_1 \Sigma_1 U_1^H + V_2 \Sigma_2 U_2^H \tag{C-21}$$

where $V_1, U_1 \in C^{n \times k}$, $V_2, U_2 \in C^{n \times (n-k)}$, $\Sigma_1 = diag[\sigma_1, \ldots, \sigma_k]$, and

The decomposition requires that inputs to the open loop system lying in the column space of U_i are amplified by the level of gain represented by the singular values and appear as outputs in the column space of V_i. This partition suggests that L be referred to as consisting of a higher gain subsystem $V_1 \Sigma_1 U_1^H$ and a lower gain subsystem $V_2 \Sigma_2 U_2^H$. The matrix $U_i^H V_j$ provides a measure of the alignment of the column spaces of U_i and V_i, and can be interpreted as a measure of interactions between the high and low gain subsystems.

Motivated by the above discussion, consider the limiting case in which $\underline{\sigma}[\Sigma_1]$ and $\overline{\sigma}[\Sigma_2]$ in the subsystem decomposition are allowed to become sufficiently large and sufficiently small, respectively. The following theorem shows that this strategy would achieve sensor noise rejection in an $(n-k)$-dimensional subspace and disturbance rejection in a k-dimensional subspace corresponding to the directions of small and large loop gain, respectively.

Theorem C-1: Let $det\left[U_1^H V_1\right] \neq 0$. Then, if

$$\underline{\sigma}[\Sigma_1] >> \overline{\sigma}\left[\left(U_1^H V_1\right)^{-1}\right]$$

(C-22)

and

$$\overline{\sigma}[\Sigma_2] << \underline{\sigma}\left[U_2^H V_2\right]$$

(C-23)

the sensitivity and complementary sensitivity matrices satisfy the following conditions:

Sensitivity matrix: $\overline{\sigma}[S - S_{app}] << 1$ and $\overline{\sigma}\left[T - T_{app}\right] << 1$

(C-24)

where

$$
\begin{aligned}
S_{app} &= U_2\left(V_2^H U_2\right)^{-1} V_2^H \\
&= U_2\left(V_2^H U_2\right)^{-1}\left(V_2^H U_1\right)U_1^H + U_2 U_2^H \\
&= V_1\left(V_1^H U_2\right)\left(V_2^H U_2\right)^{-1} V_2^H + V_2 V_2^H
\end{aligned}
$$

Complementary sensitivity matrix:
$$
\begin{aligned}
T_{app} &= V_1\left(U_1^H V_1\right)^{-1} U_1^H \\
&= U_2\left(U_2^H V_1\right)\left(U_1^H V_1\right)^{-1} U_1^H + U_1 U_1^H \\
&= V_1\left(U_1^H V_1\right)^{-1}\left(U_1^H V_2\right)V_2^H + V_1 V_1^H
\end{aligned}
$$

(C-25)

The above theorem allows feedback properties to be approximated when open loop gain is both large and small in different directions at the same frequency. However, one must take care to correctly identify the input and output directions of the high and low gain subsystems with the subspace of C^n in which the signals are to be rejected.

Next consider two additional cases: when the gain is assumed to be either (a) large in some directions or (b) small in some directions, and in each case, no assumption is placed upon gain in orthogonal directions, the following two theorems show that there exists an analogue to scalar gain crossover frequency range in which knowledge of gain alone is insufficient to allow approximation of feedback properties; hence it is necessary to consider some sort of phase information.

Theorem C-2. Let $det\left[U_1^H V_1\right] \neq 0$ and $det\left[V_2^H U_2 + \Sigma_2\right] \neq 0$. Then, if

$$\underline{\sigma}[\Sigma_1] >> max \begin{cases} \overline{\sigma}\left[\left(U_1^H V_1\right)^{-1}\right] \\ \overline{\sigma}\left\{\left(U_1^H V\right)^{-1}\left[I - \left(U_1^H V_2\right)\Sigma_2\left(V_2^H U_2 + \Sigma_2\right)^{-1}\left(V_2^H U_1\right)\right]\right\} \\ \overline{\sigma}\left\{\left(U_1^H V_1\right)^{-1}\left(U_1^H V_2\right)\Sigma_2\left(V_2^H U_2 + \Sigma_2\right)^{-1}\left(V_2^H U_2\right)\right\} \end{cases} \tag{C-26}$$

then the sensitivity and complementary sensitivity matrices satisfy the following conditions:

$$\overline{\sigma}\left[T - T_{app}\right] << 1 \text{ and } \overline{\sigma}\left[S - S_{app}\right] << 1 \tag{C-27}$$

where $S_{app} = U_2\left(V_2^H U_2 + \Sigma_2\right)^{-1} V_2^H$

and

$$T_{app} \equiv I - S_{app} = V_1\left(U_1^H V_1\right)^{-1} U_1^H + U_2\left(V_2^H U_2\right)^{-1}\Sigma_2\left(V_2^H U_2 + \Sigma_2\right)^{-1} V_2^H \tag{C-28}$$

Theorem C-3. Let $det\left[V_2^H U_2\right] \neq 0$ and $det\left[I + U_1^H V_1 \Sigma_1\right] \neq 0$. Then, if

$$\overline{\sigma}[\Sigma_2] << min \begin{cases} \underline{\sigma}\left[V_2^H U_2\right] \\ \underline{\sigma}\left\{\left[I - \left(V_2^H U_1\right)\left(I_2 + U_1^H V_1 \Sigma_1\right)^{-1}\left(U_1^H V_2\right)\right]^{-1}\left(V_2^H U_2\right)\right\} \\ 1\Big/ \overline{\sigma}\left\{\left(V_2^H U_2\right)^{-1}\left(V_2^H U_1\right)\left(I + U_1^H V_1 \Sigma_1\right)^{-1}\left(U_1^H V_1\right)\right\} \end{cases} \tag{C-29}$$

the sensitivity and complementary sensitivity matrices satisfy the following conditions:

$$\overline{\sigma}\left[S - S_{app}\right] << 1 \text{ and } \overline{\sigma}\left[T - T_{app}\right] << 1$$

where $S_{app} \equiv I - T_{app} = U_2^H\left(V_2^H U_2\right)^{-1} V_2^H + V_1\left(U_1^H V_1\right)^{-1}\left(I + U_1^H V_1 \Sigma_1\right)^{-1} U_1^H$

$$T_{app} = V_1 \Sigma_1\left(I + U_1^H V_1 \Sigma_1\right)^{-1} U_1^H \tag{C-30}$$

Remark: Theorems C-3 and Theorem C-2 show that the conditions:

$$\overline{\sigma}[\Sigma_2] \ll \underline{\sigma}\left[U_2^H V_2\right] \text{ and } \underline{\sigma}[\Sigma_2] \gg \overline{\sigma}\left[U_2^H V_2\right]$$

and the conditions:

$$\underline{\sigma}[\Sigma_1] \gg \overline{\sigma}\left[(U_1^H V_1)^{-1}\right] \text{ and } \overline{\sigma}[\Sigma_1] \ll \underline{\sigma}\left[(U_1^H V_1)^{-1}\right]$$

fail to hold at the same frequencies. Since the knowledge of the open loop singular value *gains* does not provide sufficient information to allow feedback properties to be approximated, additional information about the *phase* is necessary. This area requires further research.

In conclusion, the third approach by Freudenberg and Looze (1986), (1990), and (1988) have introduced a general concept of the relationship of the gain, phase and direction of the open loop transfer matrix with the closed-loop sensitivity and complementary sensitivity matrices. The rules developed in each of the three theorems can serve as a guide for design and robustness testing. However, more direct rules still need to be developed for robustness assessment of MIMO systems.

REFERENCES

G. J. Balas, J. C. Doyle, K. Glover, A. Packard, and R. Smith, 1991, μ-Analysis and Synthesis Toolbox - User's Guide, MuSyn Inc.

C. A. Desoer, F. M. Callier, and W. S. Chan, 1977, "Robustness Of Stability Conditions For Linear Time Invariant Feedback Systems", *IEEE Transactions on Automatic Control*, vol. AC-22, December, pp 945-949

J. C. Doyle, 1982, "Analysis of feedback systems with structured uncertainties, "*IEE Proceedings*, vol. 129, Part D, No. 6, pp. 242-250.

J. S. Freudenberg, 1990, "Plant Directionality, Coupling And Multivariable Loop-Shaping", *International Journal of Control*, vol. 51, No. 2, pp. 365-390.

J. S. Freudenberg, and D. P. Looze, 1988, *Frequency Domain Properties Of Scalar And Multivariable Feedback Systems*, Springer-Verlag.

J. S. Freudenberg, and D. P. Looze, 1986, "The Relation Between Open-Loop And Closed-Loop Properties Of Multivariable Feedback Systems", *IEEE Transactions on Automatic Control*, vol. AC-31, No. 4, pp. 333-340.

E. Kreyszig, 1972, *Advanced Engineering Mathematics*, pp. 243-253, (New York: Wiley).

T. T. Lee, and S. H. Lee, 1986, " Gain And Phase Margin For Discrete-Time Systems", *International Journal of Control*, vol. 44, No. 5, pp. 1415-1426.

N. A. Lehtomaki, N. R. Sandell, Jr., and M. Athans, 1981, "Robustness Results In Linear-Quadratic Gaussian Based Multivariable Control Designs", *IEEE Transaction on Automatic Control*, vol. AC-26, No. 1, pp. 75-92.

P. Molander, and J. C. Willems, 1980, "Synthesis Of State Feedback Control Laws With A Specified Gain And Phase Margin", *IEEE Transactions on Automatic Control*, vol. AC-25, No. 5, pp. 928-931.

C. Moler, J. Little, and S. Bangert, 1987, PC-MATLAB User's Guide, The MathWorks Inc.

A. Packard and J.C. Doyle, 1993, "The Complex Structured Singular Value," *Automatica*, Vol. 29, No. 1, pp. 71-109.

A. Packard, J.C. Doyle, J. and G.J. Balas, 1993, "Linear, Multivariable Robust Control with a μ Perspective, " *Journal of Dynamic Systems, Measurement, and Control*, Transactions of the ASME, 50th Anniversary Issue, Vol. 115, June, pp.428-438.

M. G. Safonov, and M. Athans, 1977, "Gain Margin And Phase Margin For Multiloop LQG Regulators", *IEEE Transactions on Automatic Control*, vol. AC-22, pp. 173-179.

M. G. Safonov, 1982, "Stability Margins of Diagonally Perturbed Multivariable Feedback Systems,"*IEE Proceedings*, vol. 129, Part D, No. 6, pp. 251-256.

S. Skogestad, M. Morari and J.C. Doyle, 1988, "Robust Control Of Ill-Conditioned Plants: High Purity Distillation," *IEEE Transactions on Automatic Control*, Vol. 33, No. 12, December, pp. 1092-1105.

G. Stein and J.C. Doyle, 1991, "Beyond Singular Value and Loop Shapes," *Journal of Guidance, Control and Dynamics*, vol. 14, No. 1, January-February, pp. 5-16.

C. S. Tao, C. H. Chang, and K. W. Han, 1991, "Gain Margins And Phase Margins For Multivariable Control Systems With Adjustable Parameters", *International Journal of Control*, vol. 54, No. 2, pp. 435-452.

H. H. Yeh, C. D. B. Ridgely, and S. S. Banda, 1985a, "Stability Margins Of Multivariable Feedback Systems", *Journal of Guidance, Control and Dynamics*, vol. 8, No. 2, March-April, pp. 167-175.

H. H. Yeh, S. S. Banda, and C. D. B. Ridgely, 1985b, "Stability Robustness Measures Utilizing Structural Information", *International Journal of Control*, vol. 41, No. 2, February, pp. 365-387.

H. H. Yeh, S. S. Banda, and C. D. B. Ridgely, 1984, "Regions Of Stability For Gain Or Phase Variations In Multivariable Systems", *Proceedings of 23rd Conference on Decision and Control*, Las Vegas, Nevada, December, pp. 1409-1422.

DISTRIBUTION LIST
Report No. NAWCADWAR-93010-60

No. of Copies

Defense Technical Information Center 2
ATTN: DTIC-FDAB
Cameron Station BG5
Alexandria, VA 22304-6145

Center for Naval Analyses 1
4401 Fort Avenue
P.O. Box 16268
Alexandria, VA 22302-0268

Naval Air Warfare Center 6
Aircraft Division
Warminster, PA 18974-0591
   (2 for Code 8131)
   (4 for Code 6053 - M. B. Subrahmanyam)

Control Dynamics Branch 1
Flight Control Division
Wright Laboratory
Wright-Patterson AFB, OH 45433-7562
   (1 for Dr. Siva Banda)

Office of Naval Research 1
800 N. Quincy St.
Arlington, VA 22217-5000

Department of Mechanical Engineering 20
The Pennsylvania State University
University Park, PA 16802
   (20 for Professor Asok Ray)

Naval Postgraduate School 1
Monterey, CA 93940

Office of Naval Technology 1
Arlington, VA 22217-5000